

Field Guidebook

IGCP 546

Subduction zones of the Caribbean



Subduction/accretion-related high-pressure rocks of Margarita Island, Venezuela

November 11-15, 2010

Walter V. Maresch (Ruhr-University Bochum, Germany)
Franco Urbani (FUNVISIS and Universidad Central de Venezuela)
Hans-Peter Schertl (Ruhr-University Bochum, Germany)
Klaus P. Stanek (TU Bergakademie Freiberg, Germany)

This guide has been prepared for the sole and private use of participants of the UNESCO-sponsored field trip “Subduction/accretion-related high-pressure rocks of Margarita Island, Venezuela”

Introduction

The metamorphic rocks of Margarita Island, Venezuela, have been studied and their significance debated for more than 60 years. As paradigms in the Geosciences changed, ideas guiding tectonic and geodynamic interpretations also changed. A survey of the literature on this fascinating island shows shifts from "fixist" ideas and application of classical stratigraphic nomenclature to highly metamorphosed and deformed rocks, through to interpretations calling on extreme nappe development from a classical Alpine viewpoint. Recent discussions on the origin and evolution of the Caribbean Plate, aptly summarized in an impressive compendium of 31 papers edited by James et al. (2009), underscore that understanding the geology of Margarita Island is a key element in understanding the timing and nature of interaction of the Caribbean plate with northern South America.

This field-trip, under the auspices of IUGS-UNESCO IGCP PROJECT 546 "Subduction Zones of the Caribbean", is intended to present a hands-on overview of the rocks involved in order to allow experts from other parts of the Caribbean to "get their own picture". Needless to say, the literature that has accumulated in 60 years is immense. We will base our discussion on two recent summaries by Rekowski and Rivas (2005) and Maresch et al. (2009), where much of the presently available data has been brought together. Rekowski and Rivas (2005) summarize about 100 studies including data from a number of unpublished Venezuelan theses as well as extensive tables on mineral phase assemblages and rock analyses that would otherwise be unavailable to most readers. This copious thesis is appended as a CD to this field guide. The paper of Maresch et al. (2009) is included as Appendix B. Klaus Stanek has collated and homogenized the eighteen 1:25,000 geological map sheets prepared by Rekowski and Rivas (2005) into a single geological map that will form the basis for our discussions (Plate 1). In this field guide we will follow the lithodemic nomenclature proposed by Urbani (2007, 2008) for the igneous and metamorphic units of Margarita Island (see next section). General responsibility for the ideas expressed in the following sections lies with WVM, unless otherwise indicated.

Nomenclature of the igneous and metamorphic rocks of Margarita Island, Venezuela (FU)

From 1937 to 1985 the Venezuelan Commission for Stratigraphy and Nomenclature was very active and edited the 1956 and 1970 editions of the *Venezuelan Stratigraphical Lexicon*. In 1995 the state-owned oil company PDVSA appointed Dr. Wolfgang Scherer to edit a third edition which can be consulted at www.pdvsa.com/lexico (Scherer, ed., 1997). The guidelines followed in the three editions were those of the *North American Stratigraphic Code* in their successive versions (e.g.: NACSN 1983, 2005). Despite this effort, some units of Margarita Island were omitted in the Stratigraphical Lexicon.

Due to the lack of a renewed Venezuelan Commission, in 2000 a group of active scholars from the National Geological Survey and Venezuelan universities agreed to reappraise the nomenclature of the igneous and metamorphic units of Northern Venezuela, migrating the nomenclature of Group, Formation and Member to the framework of lithodemic units, with the hierarchical order of Supersuite, Suite, Complex and lithodeme (Urbani 2008).

Almost the entire Margarita Island has been geologically mapped by students of the Universidad Central de Venezuela (UCV) between 1952 and 1983 but those works remained mostly unpublished. Fundamental works are those of the doctoral theses of Taylor (1960), Maresch (1971), Navarro (1974) and Chevalier (1987) and their follow-up publications. More recently the integration of a hundred works and maps resulted in 18 geological sheets at scale 1:25,000. It was carried out by Rekowski & Rivas (2005). These authors also compiled the numerical data of all petrographic determinations available from publications and unpublished theses. As a result of this work, the nomenclature of the units was set as shown in Table 1 (column 1).

Table 1. Nomenclature of igneous and metamorphic rock units from Margarita Island, Venezuela (All units and subunits listed in this table are mapped in the 1:25,000 sheets of Rekowski & Rivas, 2005). Indentations from left to right show units from higher to lower rank.

REKOWSKY & RIVAS (2005), in Spanish	REKOWSKY & RIVAS (2005), translated into English	Alternate version, 2010
<i>ROCAS ÍGNEAS NO METAMORFICAS</i>	<i>NON METAMORPHIC IGNEOUS ROCKS</i>	<i>NON METAMORPHIC IGNEOUS ROCKS</i>
Basalto (diques)	Basalt (dikes)	Basalt (dikes)
Diabasa (diques)	Diabase (dikes)	Diabase (dikes)
Gabro (diques)	Gabbro (dikes)	Gabbro (dikes)
Pegmatita (apófisis)	Pegmatite (apophyses)	Pegmatite (apophyses)
Volcánicas de Los Frailes	Los Frailes Volcanics	Los Frailes Basalt
<i>GRANITOIDES</i>	<i>GRANITOIDS</i>	<i>GRANITOIDS</i>
Metagranito de Cerro Boquerón	Cerro Boquerón Metagranite	Cerro Boquerón Metagranite
Metagranodiorita Agua de Vaca	Agua de Vaca Metagranodiorite	Agua de Vaca Metagranodiorite
Metagranito de El Salado	El Salado Metagranite	El Salado Metagranite
<i>ASOCIACIÓN METAMÓRFICA LOS ROBLES</i>	<i>LOS ROBLES METAMORPHIC SUITE</i>	<i>LOS ROBLES METAMORPHIC SUITE</i>
Rocas carbonáticas	Carbonated rocks	Carbonated rocks
Rocas grafitosas	Graphite rocks	Graphite rocks
Metavolcanosedimentarias	Meta-volcanosedimentary rocks	Meta-volcanosedimentary rocks
Esquisto micáceo y cuarcita	Mica schist and quartzite	Mica schist and quartzite
<i>COMPLEJO METAOFIOLÍTICO DE PARAGUACHÍ</i>	<i>PARAGUACHÍ METAOPHIOLITIC COMPLEX</i>	<i>PARAGUACHÍ SUPERSUITE</i>
Metavolcánicas de Manzanillo	Manzanillo Metavolcanics	Manzanillo Metabasalt
Metatrandjemita de Matasiete	Matasiete Metatrandhjemite	Matasiete Metatrandhjemite
Gneis de Guayacán	Guayacán Gneiss	Guayacán Gneiss
Metamáficas de La Rinconada	La Rinconada Metamafics	La Rinconada Metamafic Suite
Unidad I	Unit I	Unit I
Unidad II	Unit II	Unit II
Unidad III	Unit III	Unit III
Metagabro	Metagabbro	Metagabbro
Anfibolita	Amphibolite	Amphibolite
Esquisto anfibólico	Amphibolic Schist	Amphibolic Schist
Eclogita	Eclogite	Eclogite
Zona de cizalla (Manzanillo)	Megashear zone (Manzanillo)	Megashear zone (Manzanillo)
Metaultramáficas Cerro El Copey	Cerro El Copey Metaultramafics	Cerro El Copey Metaultramafic Suite
Serpentinita	Serpentinite	Serpentinite
Harzburgita	Harzburgite	Harzburgite
<i>ASOCIACIÓN METAMÓRFICA JUAN GRIEGO</i>	<i>JUAN GRIEGO METAMORPHIC SUITE</i>	<i>JUAN GRIEGO METAMORPHIC SUITE</i>
Mármol de El Piache (Unid. sup.)	Upper Unit (El Piache Marble)	Upper Unit (El Piache Marble)
Unidad media	Middle unit	Middle unit
Unidad inferior	Lower unit	Lower unit
Cuarcita y esquisto cuarzo micáceo granatífero	Quartzite and quartz mica garnet schist	Quartzite and quartz mica garnet schist

Maresch *et al.* (2009) comment “We see some problems with this terminology that still require clarification,... direct translation of the Spanish suggestion into English causes some linguistic problems. Thus, the direct translation of ‘Metamáficas de La Rinconada’, i.e. ‘La Rinconada Metamafics’, in which an adjective is used as a noun, would not be accepted by a number of publications.”

This objection can be overcome using the hierarchical order of supersuite, suite and lithodeme, so the rocks of the “Paraguachí Ophiolitic Complex”, can be raised to the Supersuite rank, while its constituents, as the “La Rinconada Metamafics” can be raised to the Suite rank (see Table 1, column 3).

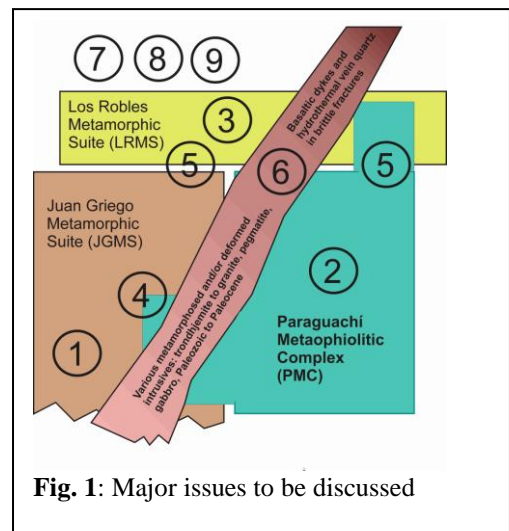
In addition, under a deeper scrutiny some of the subunits need to be modified, for instance the “eclogite” and “amphibole schist” subunits in the Macanao Península that are included in the outcrop areas of Los Robles should not be assigned to La Rinconada unit. These inconsistencies are not corrected in Table 1, but will be done in the near future since an updated edition of colored maps of Northern Venezuela is expected for 2012.

In line with Maresch *et al.* (2009), for the purpose of this field trip “the petrological content of the metamorphic rock units and not their nomenclature will be the primary objective, as well as the record and the history these rocks are telling us”. However, this field trip certainly will be a good opportunity also to discuss the nomenclature issues.

Major issues

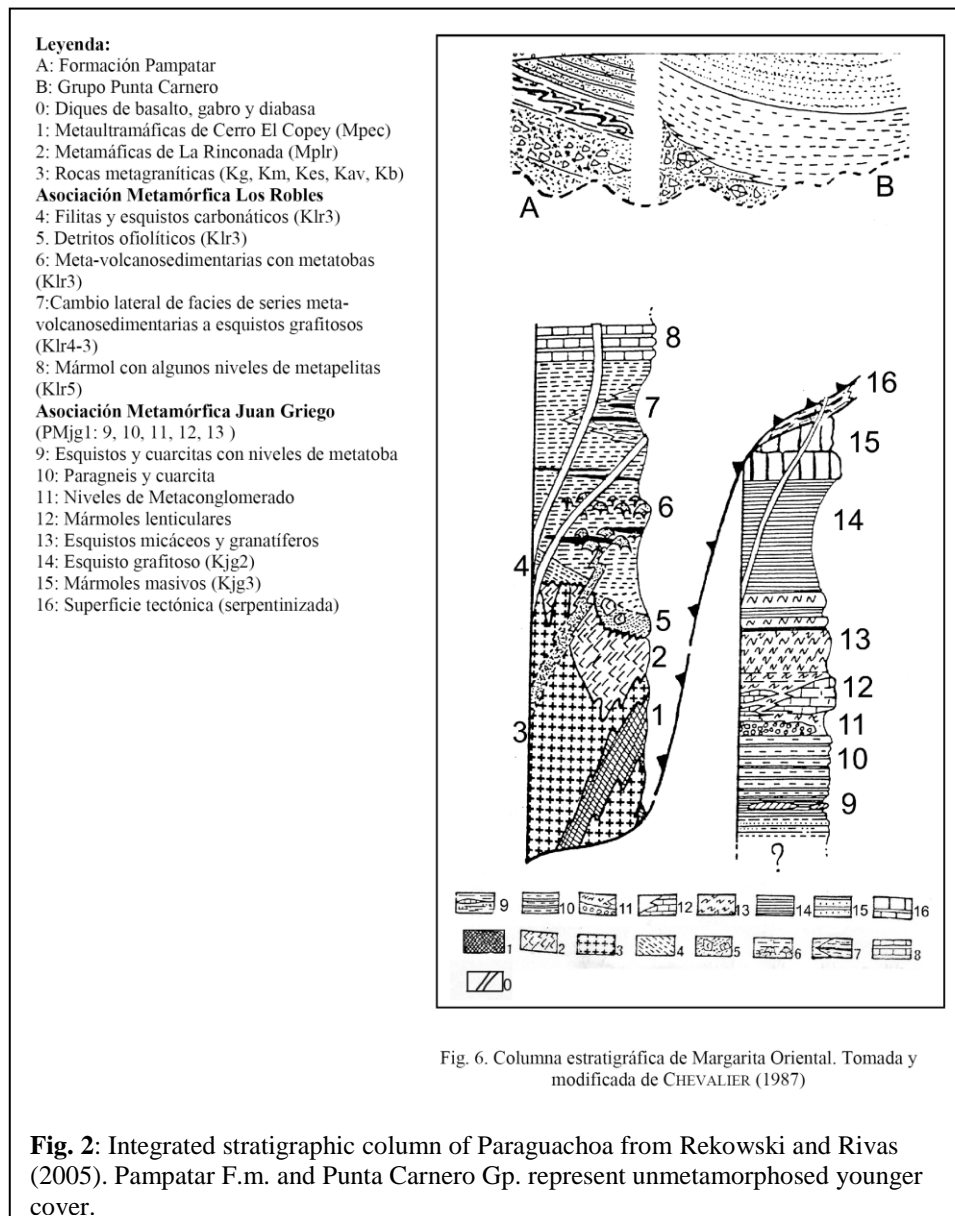
The major issues that need to be addressed in discussing the geology and tectonic history of Margarita are schematically summarized in Fig. 1. We have left out the names of the proponents of the various suggestions to emphasize neutrality.

- (1) Does the protolith of the Juan Griego Metamorphic Suite (JGMS) represent autochthonous or parautochthonous continental margin (crust + overlying sediments) of northern South America overridden by the Paraguachí Metaophiolitic Complex (PMC), or is it far-travelled material from the NW corner of South America? How much of the section is Paleozoic? How much is Mesozoic? Is it possible to define and map out a continuous sedimentary “stratigraphy” in a highly metamorphosed and isoclinally folded metasedimentary sequence?
- (2) What is the source of the PMC? MORB + underlying mantle? Is there IAT, SSZ influence? Or is it “non-ophiolitic” subcontinental mantle + theoleiitic rifted margin basalt?
- (3) What is the source of the Los Robles Metamorphic Suite (LRMS)? Is it the erstwhile regolith/sedimentary/pyroclastic cover of the PMC? Is it possible to define and map out a continuous sedimentary “stratigraphy” in a sequence with strong metamorphic gradients, thus implying parallelism of sedimentary layering and metamorphic field isograds?
- (4) What is the relationship between JGMS and PMC? Is it a major overthrust? If so, how do thrusting and high-pressure metamorphism relate in time? Is the contact an erstwhile quasi-stratigraphic, continental-margin relationship? Is it a complex formed by common accretion/metamorphism of discrete continental and oceanic units in a subduction/collision zone? What is the origin of PMC-like material in small bodies found in the JGMS: coevally metamorphosed former basaltic dykes/sills or interbedded flows/tuffs in the original



sediments; or olistoliths of PMC in continental-margin sediments. Were these olistoliths already eclogites?

- (5) What is the relationship between PMC and JGMS on the one hand and LRMS on the other? Does the LRMS represent a submarine regolith and sedimentary cover over PMC? How can the strong metamorphic contrast between LRMS and PMC be explained if both were together before HP metamorphism? Why is the sedimentary protolith of both JGMS and LRMS in part so similar?
- (6) What units do the different intermediate to acid magmatic rocks actually intrude with primary contacts? Do metatrandhjemites/metatonalites (Guayacán, Matasiete) represent MOR plagiogranites? Can they be fused former graywackes interbedded with the PMC metabasalts? Or are they adakitic products of slab anatexis? What is the relationship between granitic magmatism and the anatexitic structures found in JGMS gneisses? Is the anatexis Paleozoic (old basement) or Mesozoic (i.e. subduction-related)?
- (7) Do the distinctive nappe structures postulated for Margarita agree with metamorphic field gradients? How many high-pressure metamorphic events are recorded on Margarita?
- (8) How can the available data be integrated into regional geodynamic models of the Caribbean?
- (9) What additional problems and/or answers will the assembled experts on Caribbean geology think of?

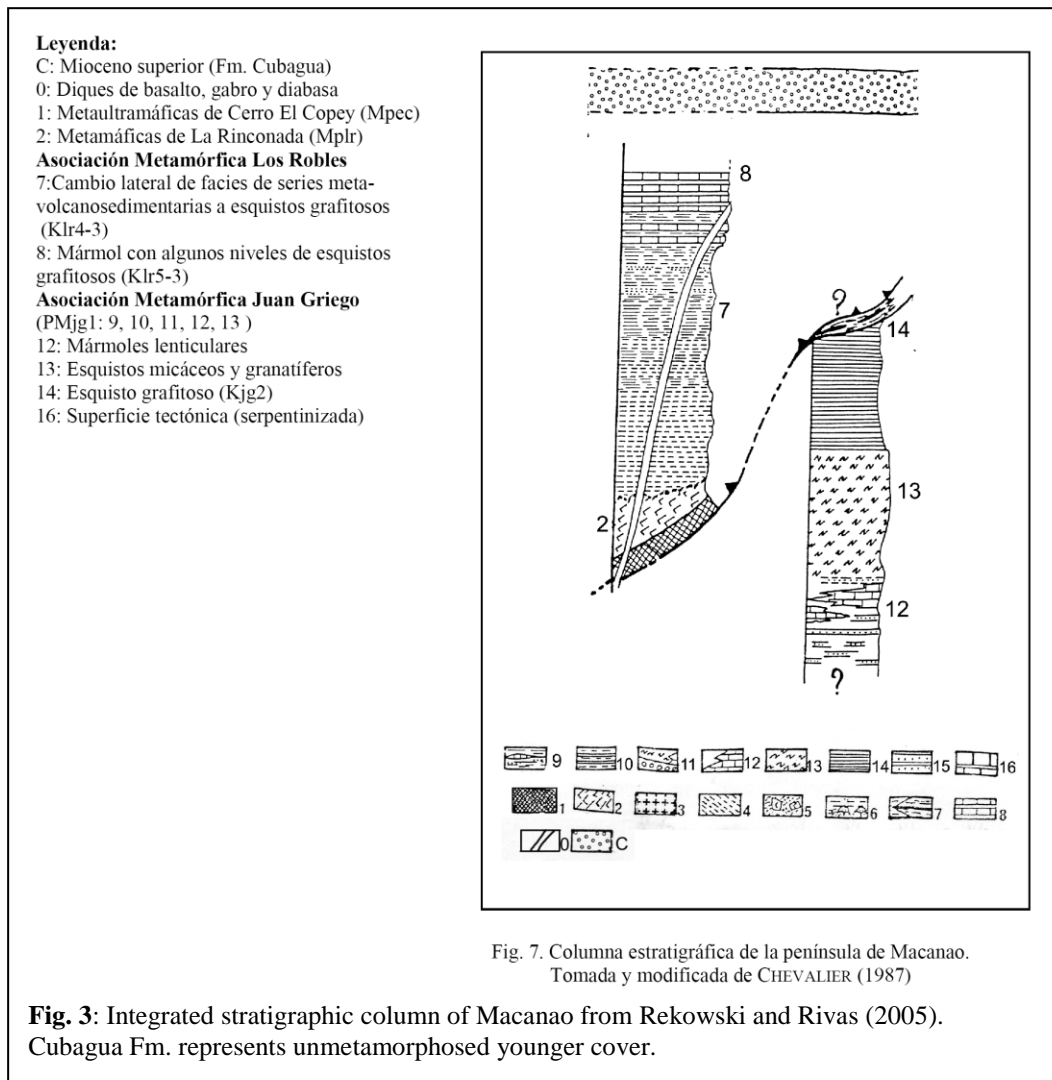


Protoliths

Rekowski and Rivas (2005, Appendix A, attached CD) as well as Maresch et al. (2009; Appendix B) have summarized and discussed present ideas on the protoliths of Margaritas metamorphic rocks in considerable detail. We restrict ourselves to a brief overview here.

There is a general consensus that the JGMS is of continental affinity (probably continental basement and overlying sediments) whereas the PMC is oceanic in character, with peridotite, basalt and only minor graphitic metasedimentary interlayers. The origin of the LRMS (composed of heterogeneous metasediments, marbles, and intermediate to basic metaproclastic/metavolcanic deposits) is less clear.

Based mainly on the work of Chevalier (1987), Rekowski and Rivas (2005) have suggested integrated stratigraphic columns for Paraguachoa (Fig. 2) and Macanao (Fig. 3), in which the main lithotypes involved are indicated. Reference should also be made to the legend of the geological map in Plate 1. Note that these columns follow the hypothesis of Chevalier (1987) and Chevalier et al. (1988) of a major thrust boundary between JGMS and MPC, an assumption that is strongly contested by Maresch et al. (2009). Note also that these columns show that all intermediate to acid intrusives are restricted to the allochthonous PMC, a conclusion at variance with evidence presented by Maresch et al. (2009).



The JGMS sequence consists of a lower part in which gneiss and quartzite predominate, with a higher section more rich in various types of mica-schist. Marbles occur. Dated orthogneiss from Macanao (Maresch et al, 2009) has been taken to indicate Paleozoic ages for the lower parts of the section (Rekowski and Rivas, 2005) with Cretaceous ages assumed for the upper sequences.

However, it should be noted that detrital zircon age data (Wright, pers. commun., 2010) from paragneiss mapped as PM_{JG} near Juan Griego indicate Lower Cretaceous ages. Both Chevalier (1987; see also Chevalier et al., 1988, Rekowski and Rivas, 2005) and Maresch et al. (2009) assume that this sequence represents South American continental crust and overlying sediments, but differ in the location of this incorporated “passive margin”. Whereas Chevalier (1987) speaks of a parautochthonous overridden margin in essentially its present location, Maresch et al. (2009) point out that there is no evidence of a connection of the JGMS with the present South American craton. Indeed, recent geophysical studies indicate that Margarita is isolated and “floating high” on the Caribbean plate. Detrital zircon age data (Wright, pers. commun., 2010) indicates that the JGMS zircon suite shows significant differences w.r.t. cratonic Guayana and appears to contain a source originating from the Venezuelan or northern Colombian Andes.

As discussed by Maresch et al. (2009), tonalitic to granitic intrusives punctuate the geological history of Margarita Island and indicate a more heterogeneous magmatic sequence than suggested in Figs. 1 and 2. The tonalites/trondhjemites of the Guayacán Gneiss intruded at 116–106 Ma and pre-date high-pressure metamorphism. Maresch et al. (2009) present evidence that these magmas intruded both the JGMS as well as the PMC. Therefore the two units must have been together before the high-pressure event. The magmas of the El Salado Metagranite intruded at ~ 86 Ma and show no evidence of the high-pressure metamorphism, thus bracketing this event in time. Despite these clarifications, there are a number of additional intermediate to acid intrusives on Margarita Island that have not been studied in detail and will require further work. We will visit several examples on our trip.

Present large-scale structure of Margarita Island

Present ideas on the structure of Margarita Island demonstrate two conflicting trains of thought. Early systematic mapping 40 years ago was characterized by the constraints imposed by the call for strict adherence to the guiding stratigraphical principles of the time, even though the pre-

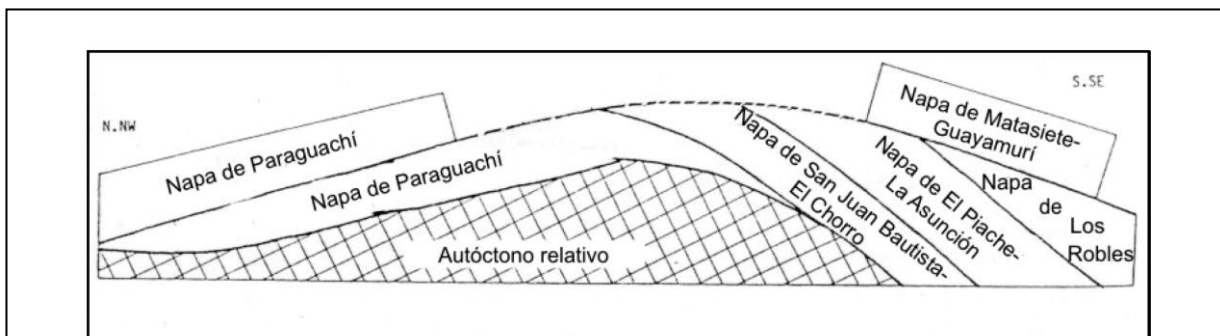


Fig. 46. Corte esquemático de las nappas de Margarita Oriental. Tomado y modificado de CHEVALIER (1987)

Fig. 4: Nappe structure of eastern Margarita Island taken from Rekowski and Rivas (2005). The eight nappes postulated by Chevalier (1987) have been simplified and reinterpreted. Nappe development is considered to have occurred during the Senonian, i.e. ~ 80 Ma (Chevalier, 1987; Chevalier et al., 1988)

Tertiary rocks were strongly deformed and clearly metamorphosed. Chevalier (1987) reinterpreted the gross structure of the island in terms of a nappe stack analogous to Alpine examples. In this context Chevalier (pers. commun., 2008) used as one of his guides the principle that serpentinite lenses found in metamorphic sequences can be interpreted to define major nappe boundaries and can be regarded as lubricants at the base of allochthonous units. Chevalier (1987) interpreted the structure of Margarita in terms of extreme nappe development and postulated at least eight nappes that are considered to dissect the metamorphic section on Margarita Island (see Fig. 4). Lying on top of the relative autochthon represented by the JGMS (i.e. South American continental margin), Chevalier (1987) postulated a lower nappe stack truncated by overlying nappes characterized by lower grades of metamorphism originating from the most

external domains of the orogen. Fig. 4 is a schematic representation of this structure for eastern Margarita. Only the autochthonous basement and the Los Robles nappe are found on Macanao. These nappes are shown in outcrop distribution in the inset to the geological map of Rekowski and Rivas (2005) on Plate 1.

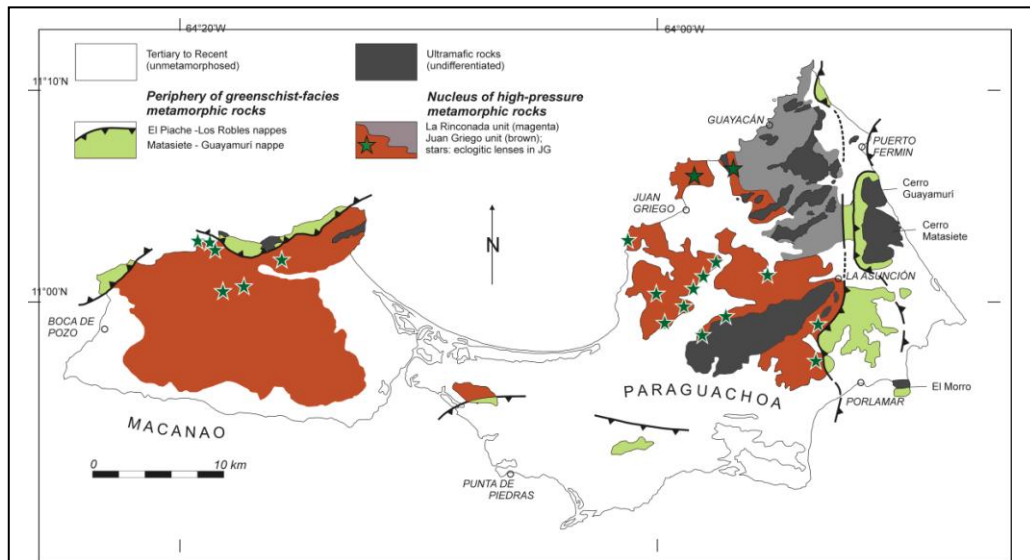


Fig. 5: Distribution of rocks of the HP nucleus and the greenschist-facies periphery on Margarita Island (adapted from Maresch et al., 2009).

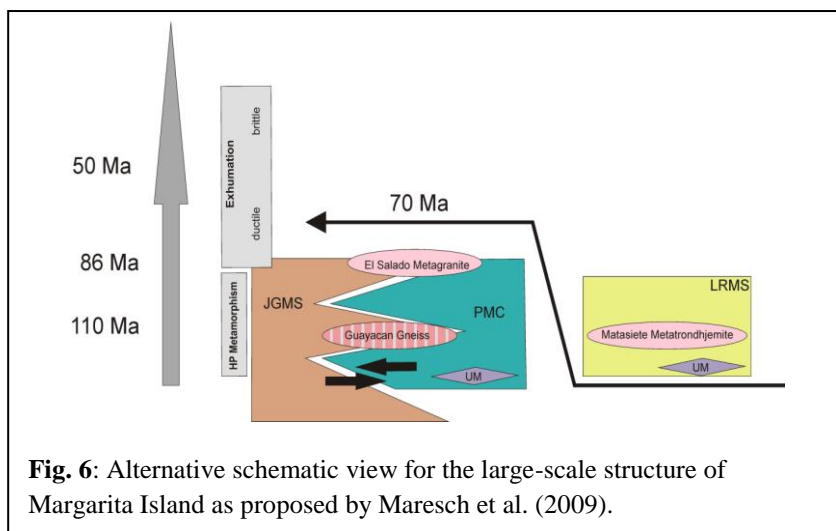


Fig. 6: Alternative schematic view for the large-scale structure of Margarita Island as proposed by Maresch et al. (2009).

However, Maresch et al. (2009) point out that this nappe structure disagrees in important aspects with the distribution of the metamorphic grades and pressure-temperature-time-deformation paths observed on Margarita (see following sections). It has been known since the work of Maresch (1971, 1973, 1975, 1977), that the metabasic sequence of NE Margarita represents a classical example of a

continuous metamorphic field gradient leading from epidote-amphibolite grade to eclogite grade. There is no break in this gradient to substantiate the existence of a major duplex structure (originally defined as a nappe boundary by Chevalier, 1987) as implied for the Paraguachí nappe. On the other hand, many of the postulated nappes (including the so-called autochthonous basement!) possess comparable metamorphic grades and similar pressure-temperature-time-deformation paths. Their juxtaposition, whether as nappes or ductile imbrications in an accretionary complex would then have to have taken place *prior* to peak high-pressure metamorphism. For these reasons, and because the common high-pressure metamorphic history is the key element in interpreting the geodynamic history of Margarita, Maresch et al. (2009) suggest defining a core or nucleus of metamorphic rocks with a similar high-grade metamorphic history from a periphery that has not exceeded greenschist grade (Fig. 5). This alternative view of the large scale structure is shown schematically in Fig. 6.

Structural development

A number of structural studies have been carried out on Margarita Island. These have been compiled by Rekowski and Rivas (2005), whose tabulated comparison is reproduced in Table 2.

Table 2: Summary of structural studies carried out on Margarita Island. Taken from Rekowski and Rivas (2005).

		Autores		
		VIGNALI (1972, 1979)	GUTH & AVÉ LALLEMANT (1989)	CHEVALIER (1987), CHEVALIER <i>et al.</i> (1995)
Fases de deformación	Fase 1	f1 Pliegues isoclinales. Metamorfismo de alto grado.	D1a Foliación en los boudines (Knockers) de eclogita. Desarrollado en la facies de la eclogita	
	Fase 2	f2 Sincrónica con el metamorfismo de la facies de la anfibolita epidótica – esquistos verdes. Genera foliación predominante, la cual es paralela a los planos axiales de los pliegues isoclinales (flancos atenuados y las partes apicales engrosadas)	D1b Sincrónica con el metamorfismo de la facies de la anfibolita epidótica y esquistos verdes. Genera foliación predominante, la cual es paralela a los planos axiales de los pliegues isoclinales D1c Facies de los esquistos verdes Deformación extensional SW-NE	D1S1 Foliación regional S1 L1: Margarita Oriental: N-NE y en la península de Macanao: E – NE. Metamorfismo variable entre la facies de la eclogita y la facies de los esquistos verdes Estructuras plegadas P1, con ejes paralelos a la dirección de alargamiento mineral L1 (pliegues en forma de “dedo”)
	Fase 3	(f3) Pliega la foliación metamórfica (f2) así como las capas en el flysh Eoceno y las pegmatitas de Macanao, afecta de modo regional los planos de foliación.	D2 Pliega la foliación generada en D1b, genera un mega-antiforme con dirección NE-SW con vergencia NW y declive al SW	D2S2 Estructuras previas son deformadas por P2 P2: pliegues rectos a levemente volcados al SE La intersección de S1 y S2, es paralela a la dirección L1. Relacionada con un sistema de fallas inversas o corrimientos.
	Fase 4		D3 Deformación de dominio frágil. Produce extensión SW-NE	

Although there are differences in detail, there is obviously a general consensus concerning the major features involved. Phases 1 and 2, as defined by Rekowski and Rivas (2005), reflect deformation during metamorphism, beginning with high-grade eclogite facies conditions evolving through upper-greenschist to lower-greenschist conditions during exhumation into the brittle regime. No neoblastesis, especially of white mica, is observed during phase 3. Phase 4 is entirely confined to the brittle field. Stöckhert *et al.* (1993) presented a schematic summary for better visualization (reproduced in Fig. 7). An initial deformational phase produced a foliation that is subsequently refolded. High-pressure metamorphic conditions outlasted this refolding. A subsequent major ductile phase during greenschist-facies conditions produced a pervasive, now ENE-WSW subhorizontal stretching lineation with parallel fold axes. This latest ductile deformation is responsible for the present ENE-WSW grain of the island. It is most prominent in quartz-rich rocks and has obliterated the high-pressure record in most of these.

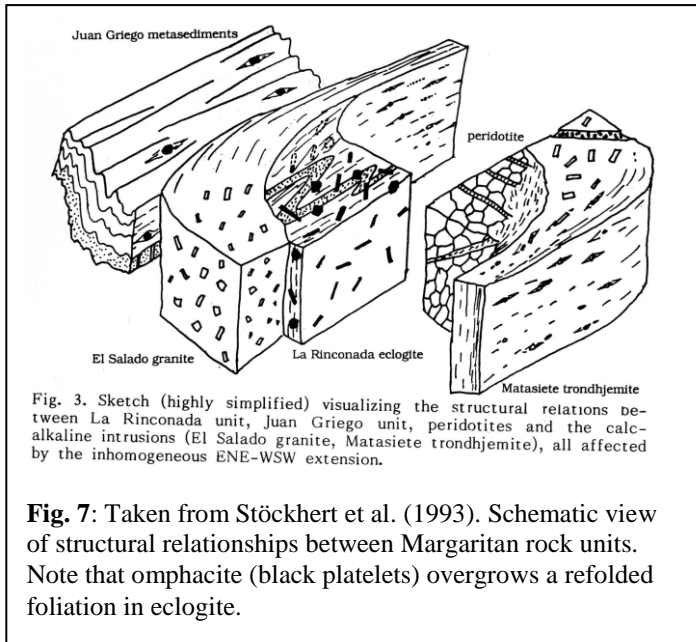


Fig. 7: Taken from Stöckhert et al. (1993). Schematic view of structural relationships between Margaritan rock units. Note that omphacite (black platelets) overgrows a refolded foliation in eclogite.

Chevalier (1987) correlated the relative development of metamorphic mineral assemblages and the change from ductile (“s-type”-dominated) to brittle (“c-type”-dominated) deformation in “meta-ophiolites” (PMC) and deracinated (uprooted) JGMS. Although Chevalier (1987) did not specifically recognize high-pressure assemblages in the JGMS, he noted the striking similarity in qualitative metamorphic development between PMC and JGMS.

Metamorphism in rocks of the high-pressure nucleus

P-T-t paths and metamorphic field gradient in schists and gneisses of the JGMS:

The study of Krückhans-Lueder (1996) first showed conclusively that the metapelites of the JGMS have a high-pressure metamorphic history that is comparable to that of the eclogites of the PMC. This obviates the problem of explaining the existence of eclogite bodies in schists and gneisses that were assumed never to have exceeded epidote-amphibolite to greenschist-facies grade (Rekowski and Rivas, 2005), and lays to rest a number of adventurous suggestions that grace the literature on this subject. Krückhans-Lueder (1996) found Al-rich metapelites with low-variance mineral assemblages including kyanite, staurolite, garnet, phengite, chloritoid, etc., that allowed accurate thermobarometry as well as qualitative chemographic analysis. Fig. 9 summarizes these data and quantifies the exhumation path implied in Fig. 8. For further details see Appendix B.

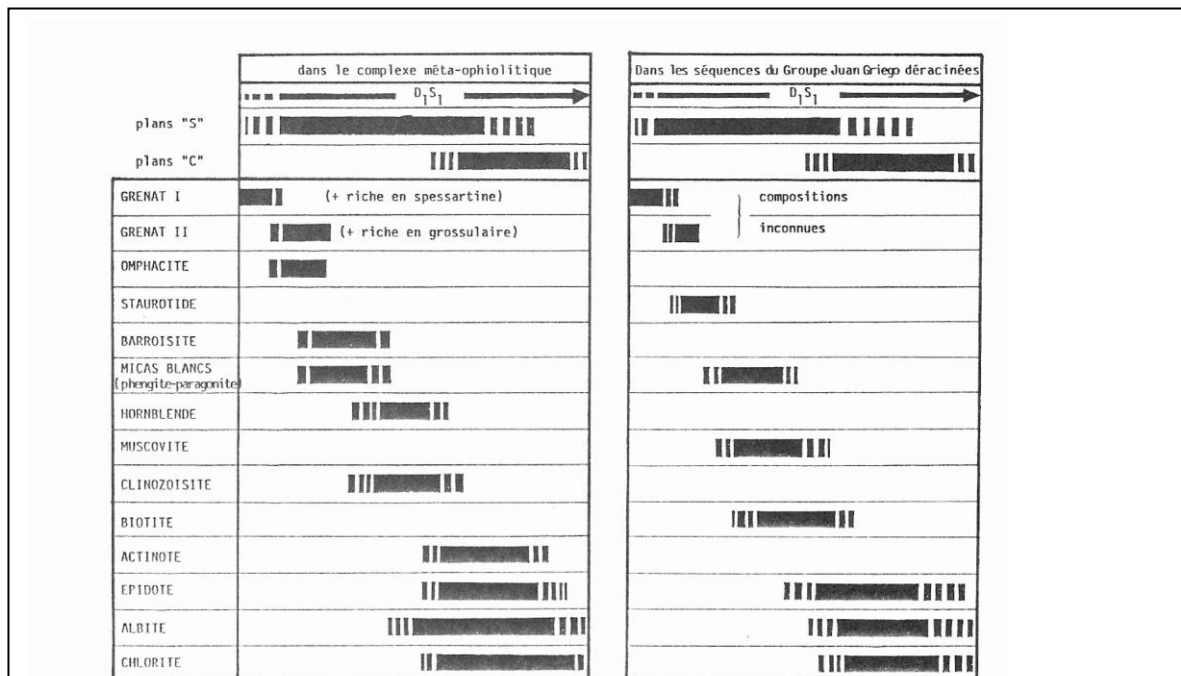
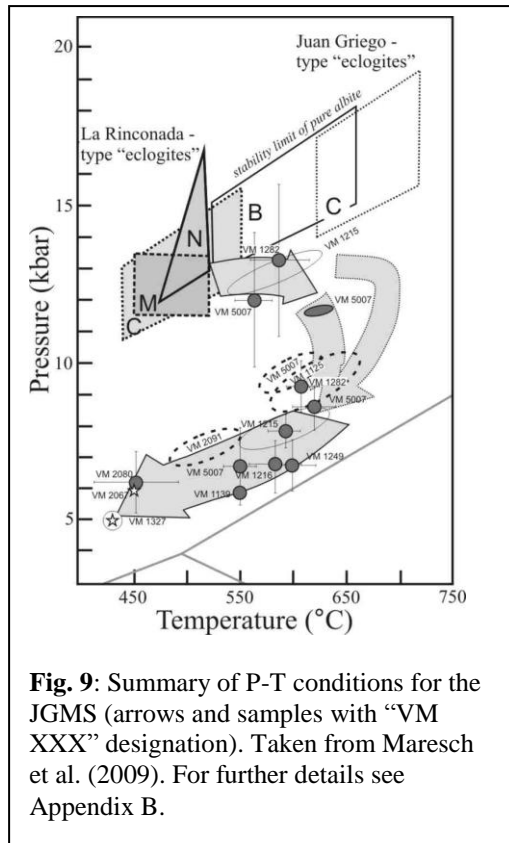


Fig. 160 - Tableau schématique illustrant les relations entre la déformation D_1S_1 et le métamorphisme M_1 dans les unités inférieures de l'ensemble supérieur à Paraguachoa. Cuadro esquemático ilustrando las relaciones entre la deformación D_1S_1 y el metamorfismo M_1 dentro las unidades inferiores de la unidad superior aloctona en Paraguachoa.

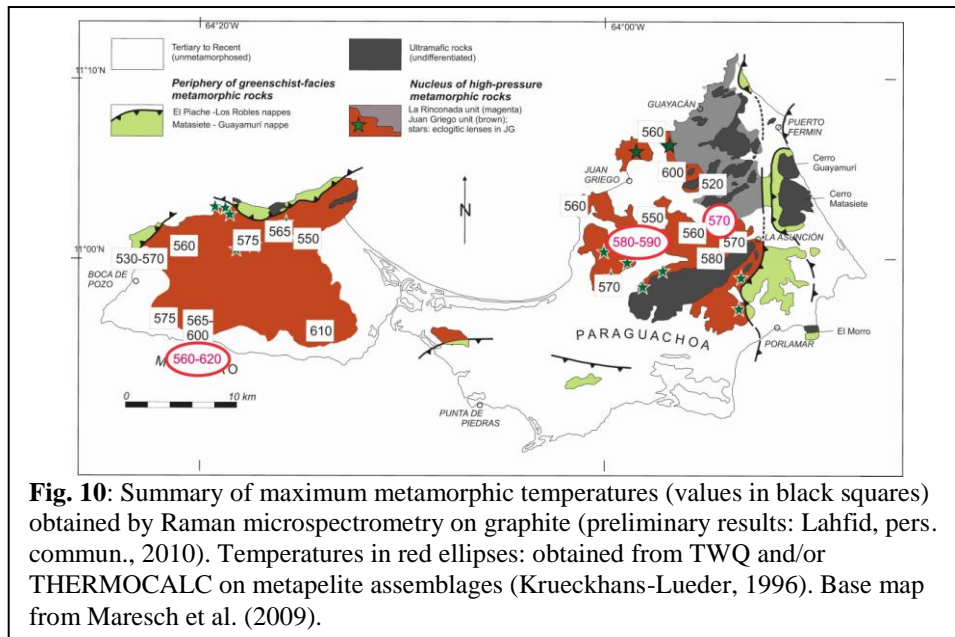
Fig. 8: Linked development of metamorphism and deformation in PMC- and JGMS-type rocks. Taken from Chevalier (1987).

The study of Krükhans-Lueder (1996) is a step in the right direction, but more P-T-t data are needed to truly understand the nature of the obviously very heterogeneous JGMS. Robust thermobarometry requires time-consuming accurate petrographical and microanalytical work



before any calculations can be attempted. Fig. 10 summarizes some preliminary data we have obtained by micro-Raman spectrometry of graphite in metasediments (Beysac et al., 2002). Carbonaceous material (CM) in the initial sedimentary rock progressively transforms into graphite (graphitization) as a function of both time and temperature. Given comparable durations of metamorphic influence, the progressive evolution of the degree of crystallinity of the CM can be used to gauge metamorphic grade. The method is comparatively quick. Because of the irreversible character of the graphitization process, the CM structure is not sensitive to retrograde metamorphism and therefore yields primarily the maximum temperature reached. Different degrees of deformation do not seem to significantly affect the structural organization of the CM. Calibrations are available for the temperature range 330-650°C (Beysac et al., 2002), but because of uncertainties in the available petrological data used for calibration, the absolute temperature uncertainties are at present $\pm 50^\circ\text{C}$. The relative uncertainties are much smaller, perhaps as low as $\pm 10^\circ\text{C}$ (Beysac, pers. commun., 2006).

Although the results are still to be considered as preliminary, Fig. 10 indicates that the maximum temperatures reached in the JGMS are very uniform, ranging on an average between 550 and 600°C. These temperatures agree well with thermobarometric determinations based on multi-equilibria calculations (TWQ, THERMOCALC, indicated in Fig. 10), but are somewhat lower



than those derived from classical approaches such as garnet-phengite thermometry (Krükhans-Lueder, 1996) incorporated in Fig. 9. The results argue for a relatively homogeneous metamorphic grade for the whole of the JGMS outcrop area. Whether the indicated trend to higher temperatures in southern Macanao, or the single low temperature (520 °C) from graphitic schist within the PMC outcrop area are robust results will have to be seen in the future.

Metamorphic field gradient and P-T-t paths of metabasic rocks

Metamorphic field gradient in NE Paraguachoa (La Rinconada outcrop area):

Maresch (1971, 1973, 1975) mapped three metamorphic zones in the basic rocks of the La Rinconada outcrop area between El Portachuelo in the south and Cabo Negro in the north, based on the appearance of paragonite and omphacite in these barroisite-rich assemblages (Fig. 11). These zones indicate a systematic increase, predominantly in pressure, from south to north. The changes in mineral assemblages and the reactions responsible for them can be summarized as shown in Table 3. They are best visualized in terms of a schematic projection from epidote and garnet (as well as SiO₂ and H₂O) as shown in Fig. 11.

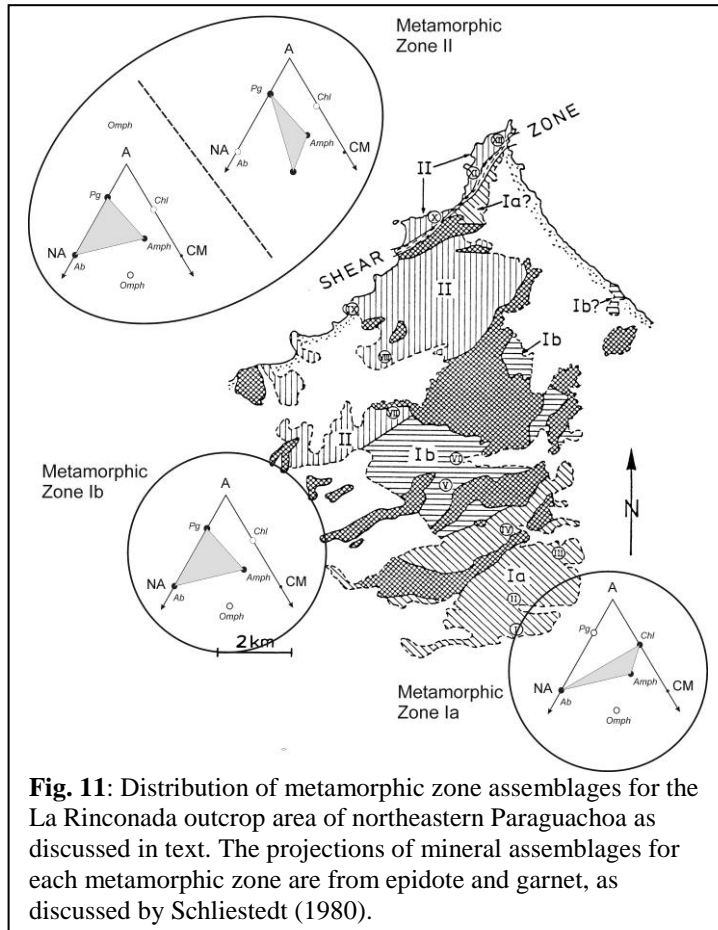
Only those mineral assemblages with the lowest variance (i.e. with the maximum number of minerals coexisting in equilibrium) are listed. Subsets of these assemblages are possible. Nevertheless, given a tholeiitic bulk composition, metamorphic zone Ia is characterized by the presence of chlorite and the lack of paragonite and omphacite, zone Ib by the appearance of paragonite at the expense of chlorite, and zone II by the appearance of omphacite at the expense of albite. The assemblage of zone Ia can be considered typical of high-pressure epidote amphibolites, while zone II represents the eclogite facies. Zone Ib represents an intermediate P-T region characterized by the coexistence of barroisite with paragonite. This intermediate assemblage between the epidote-amphibolite and eclogite facies is analogous to the paragonite-bearing amphibolites described by Konzett and Hoinkes (1996) from the Austroalpine Schneeberg Complex, Southern Tyrol.

Table 3: Summary of low variance mineral assemblages and reactions relating them in the La Rinconada outcrop area of NE Paraguachoa.

NORTH	
	<i>Lowest variance mineral assemblages</i>
Metamorphic Zone II	barroisite + garnet + epidote + omphacite + paragonite + quartz (± phengite + rutile/sphene)*
<i>projected reaction, zone Ib → II</i>	<i>barroisite + albite (+ epidote) → omphacite + paragonite (+ garnet + quartz + H₂O)</i>
Metamorphic Zone Ib	barroisite + garnet + epidote + albite + paragonite + quartz (± phengite + rutile/sphene)*
<i>projected reaction, zone Ia → Ib</i>	<i>albite + chlorite (+ epidote) → paragonite + barroisite (+ garnet + quartz + H₂O)</i>
Metamorphic Zone Ia	barroisite + garnet + epidote + albite + chlorite + quartz (± phengite + rutile/sphene)*
(* presence or absence of phengite is dictated by bulk rock K ₂ O content; rutile/sphene relationships have been neglected)	
SOUTH	

Notwithstanding the difficulties of systematically and routinely distinguishing paragonite from phengite (staining procedures help!) and recognizing secondary chlorite, the Ia - Ib boundary appears well-defined. On the other hand, the Ib - II boundary is gradational. Maresch (1971, 1973, 1975) placed the boundary at the southernmost limit of omphacite appearance. The reason for the coexistence of both type Ib (without omphacite) and type II (with omphacite) assemblages in metamorphic zone II, i.e. at presumably similar pressures and temperatures, is still not entirely clear. Mottana et al. (1985) found no obvious differences in bulk composition between rocks with or without omphacite, although more systematic work appears warranted. The fact that the amount of omphacite can be quite variable in these rocks seems to imply a certain degree of bulk compositional control. On the other hand, reaction Ib → II (Table 3) appears to be a low-variance discontinuous reaction in pressure and temperature. The omphacite-rich assemblages occur mainly in coarse-grained, sill-like bodies in the metabasaltic sequence, whereas the omphacite-poor or omphacite-free rocks are mainly found in more finely laminated

metabasaltic rock types. Navarro (1974) called these coarse-grained tabular eclogitic bodies the “Pedro-Gonzalez type” to differentiate them from the eclogitic boudins found in the Juan Griego unit (called “Macanao type” by Blackburn and Navarro, 1977). Maresch (1977) and Maresch and Abraham (1977, 1981) speculated that variable water activity could be an explanation, with low $a(\text{H}_2\text{O})$ in competent coarse-grained gabbroic rocks leading to omphacite at lower pressures than in the enclosing more permeable, fine-grained basaltic sequences. However, no diagnostic fluid inclusions were found. Selverstone et al. (1992) have documented highly variable $a(\text{H}_2\text{O})$ on the scale of millimeters to centimeters in banded mafic eclogites of the Tauern Window, Austria, lending some credence to this working hypothesis, but the Tauern Window sequence also includes carbonate-rich layers (dolomite) so far not observed in the La Rinconada rocks.



amphibole must always have been a major constituent of these rocks, and *true* eclogites are indeed extremely rare on Margarita Island. Although it is conceivable that amphibole eclogites and assemblages lacking omphacite might represent different stages of retrogression coexisting side by side, such retrogression usually produces very clear reaction textures that are not observed in most amphibole schists and gneisses lacking omphacite (see below). At present, we suggest that a systematic modern chemographic or “pseudosection” analysis is clearly called for to assess these problems.

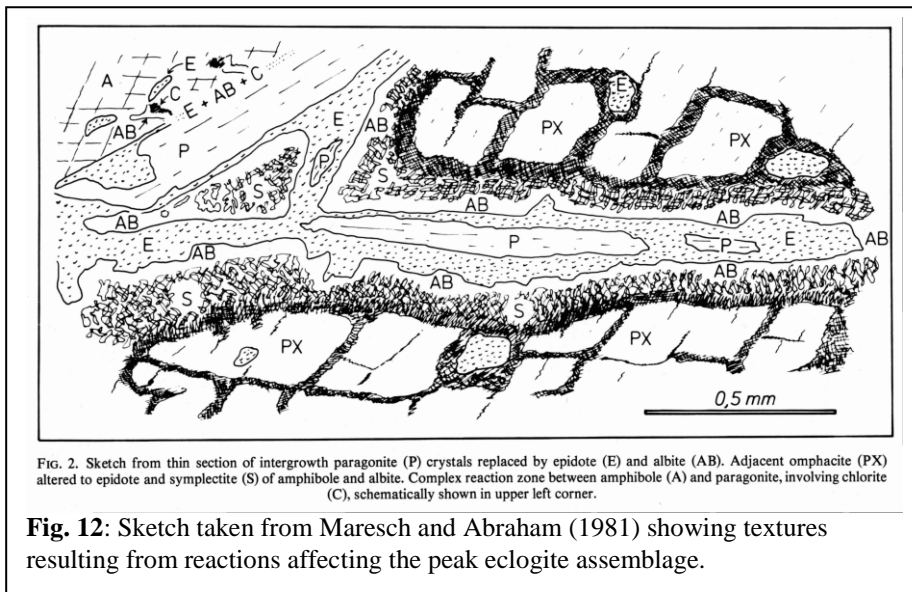
The key feature is that the La Rinconada metamorphic profile appears strongly pressure-dependent and provides a case study for the transition from the epidote-amphibolite to the eclogite facies. Molina and Poli (1998) have summarized data from similar areas and discussed these in terms of a chemographic analysis of high-pressure mafic rocks from the Nevado-Filábride Complex (SE Spain). They conclude that a reaction analogous to $\text{Ib} \rightarrow \text{II}$ accounts for the transition from the amphibolite to the eclogite facies. This reaction has a low P-T slope and at 500 – 600°C should lie between 10-15 kbar. Given that the P-T calculation of Newton (1986; see Fig. 9) for an amphibole-paragonite eclogite from Pedro González (Maresch and Abraham, 1981) is arguably the best available estimate for this eclogite (see next section), then Newton’s data of 475-525°C and ~ 12 – 17 kbar fits the conclusions of Molina and Poli (1998) well.

An alternative explanation is given by Navarro (1974, 1981) and Blackburn and Navarro (1977), who suggest that all these eclogitic rocks are the result of “various stages of transformation from eclogites through amphibole eclogites and garnet amphibolites to garnet-free diablastic amphibolites”. Actually, normal tholeiitic bulk compositions should not lead to bimineralic garnet-clinopyroxene assemblages in low to medium-T eclogites (Carswell, 1990). Rudolph (1981) tested this hypothesis for five Macanao-type amphibole eclogites by calculating theoretical modes on the basis of bulk-rock analyses and analyzed mineral compositions for each rock. He found that garnet + omphacite could account for only 58 to 78% of the rock, whereas amphibole amounted to between 22 and 40%, thus leading to totals of 92 – 98%. Excess Al_2O_3 , $\text{FeO}_{\text{total}}$ and CaO can be logically assigned to an epidote-group mineral. Thus

Similarly, the pressures of ~ 9 - 11 kbar or 8 – 10 kbar deduced by Molina and Poli (1998) and Konzett and Hoinkes (1996), respectively, for paragonite-bearing amphibolites provide a logical intermediate step between the epidote amphibolites of metamorphic zone Ia and the eclogites of metamorphic zone II. The systematics of changing phase assemblages in the La Rinconada outcrop area argue against the existence of any major nappe structures post-dating the establishment of this metamorphic field gradient (cf. Chevalier, 1987; Rekowski and Rivas, 2005).

Exhumation P-T-t paths in NE Paraguachoa (La Rinconada outcrop area):

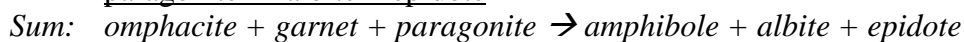
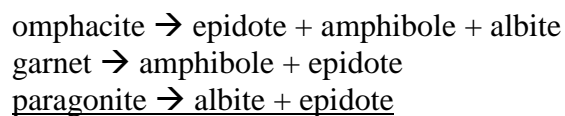
Many workers who have examined eclogites from Margarita have noted that omphacite is rarely fresh. Fine-grained symplectites consisting of albite and amphibole replace omphacite at crystal edges and along cleavage planes. However, these are not the only reactions observed altering the peak eclogite assemblage. White mica and garnet are also affected (Figs. 12, 13). Blackburn and



Navarro (1977) noted that many garnets have chemically distinct outer rims that signal late reactions with the rock matrix. Maresch and Abraham (1977, 1981) noted partial replacement of garnet by amphibole and epidote. Maresch (1971, 1973) and Maresch and Abraham (1977, 1981) also pointed out that paragonite is replaced by albite, epidote and

chlorite leading to distinctive pseudomorphs (Fig. 12). Navarro (1974, 1977) interpreted these features as clinozoisite/albite/paragonite pseudomorphs after lawsonite, i.e. reflecting an early stage in eclogite history, but the shape of the pseudomorphs is mica-like and platy rather than exhibiting the rectangular cross-sections typical of lawsonite. In addition, all stages of paragonite transformation can be observed.

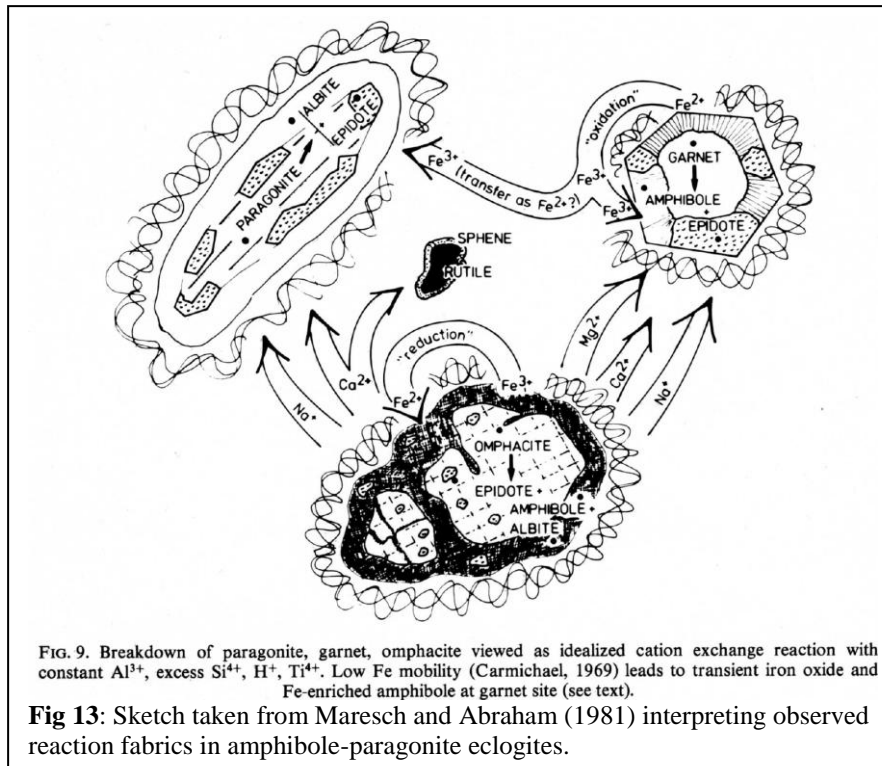
None of the reactions affecting omphacite, garnet and epidote are isochemical, and Maresch and Abraham (1977, 1981) showed that by assuming Al^{3+} to be the least mobile cation (Carmichael, 1969) the following summary reaction can be constructed (Fig. 13):



Comparison with Table 3 shows that this reaction is analogous to the zone II → Ib boundary. In addition, amphibole-paragonite contacts (upper left in Fig. 12) in zone II and in zone Ib assemblages are festooned by the reaction assemblage albite + chlorite + epidote, so that the zone Ib → Ia reaction has also been overstepped in the late history of the eclogite. In addition (Maresch, unpubl. data), it can be shown that the barroisite in all three zones is replaced along rims by hornblende *s.l.*. These observations corroborate an essentially isothermal uplift path in which all rocks of the La Rinconada sequence achieved a P-T-regime typical of the epidote amphibolite facies.

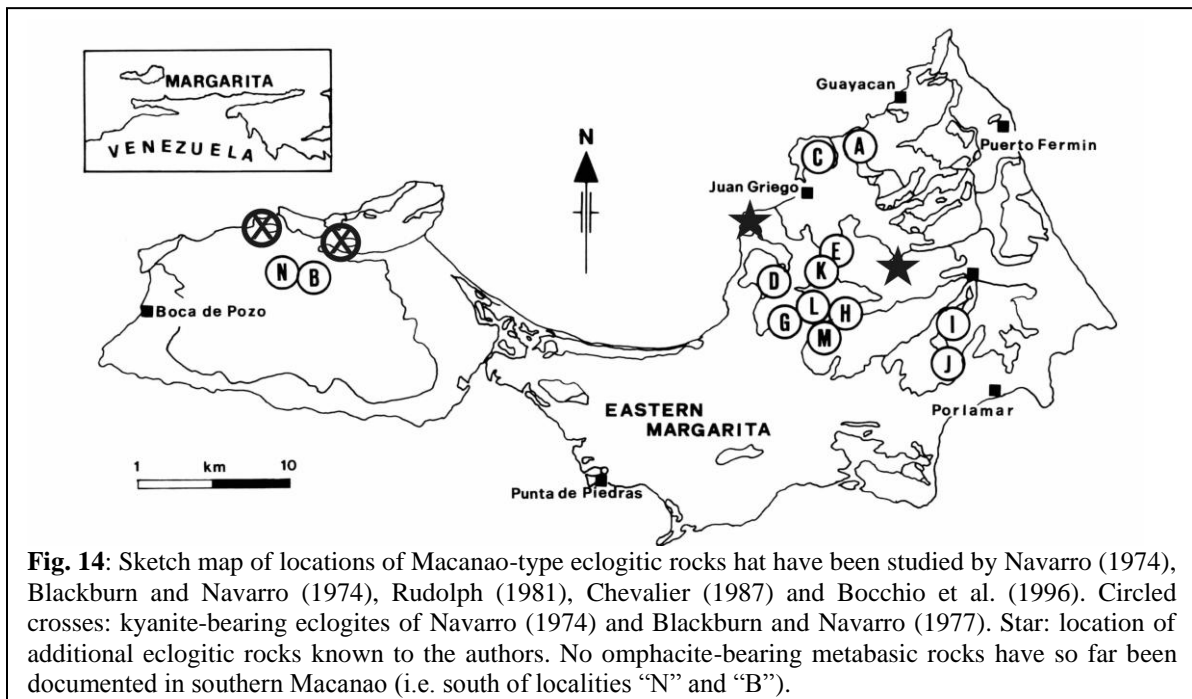
Metamorphic history of the Macanao-type eclogites:

Whereas the metabasic rocks of the La Rinconada unit appear to represent a relatively coherent sequence with a coherent metamorphic history, each of the many small pods and boudins of eclogitic rock dispersed throughout the Juan Griego outcrop area presents an individual problem in thermobarometry (Navarro, 1974, 1977, 1981, 1997; Blackburn and Navarro, 1977; Rudolph, 1981; Chevalier, 1987; Bocchio et al., 1996).



Classical methods are error-prone, and the ranges in temperature and pressure so obtained are broad (see Fig. 9). Temperatures are usually estimated from the Fe^{2+}/Mg fractionation between omphacite and garnet. However, the various calibrations of the distribution coefficient can lead to differences in temperature of 100° or more. In addition, Fe^{2+}/Fe^{3+} ratios must be calculated for garnet and especially for omphacite from stoichiometric

considerations. All analytical uncertainties will accumulate in the result and propagate into the calculated temperatures. Because garnet rarely encloses omphacite during growth, it is a common but necessarily oversimplified procedure to correlate core compositions of omphacite



and garnet to obtain data on the prograde path of the rock (e.g. Navarro, 1981, 1997; Chevalier, 1987; Bocchio et al., 1996). The fact that garnet is commonly zoned but omphacite is not represents a clear signal for the dangers in this approach. Pressures are usually estimated from the jadeite content of omphacite, but these are minimum pressures only. The time therefore

appears ripe to apply modern techniques of multi-equilibrium calculations and isochemical P-T diagrams (“pseudosections”) using internally consistent thermodynamic data sets. Newton (1986) applied an internally consistent data set to the analytical data of Maresch and Abraham (1981) and provided a first robust result for an amphibole-paragonite eclogite from Pedro Gonzalez (see Fig. 9).

Systematic microanalytical data for eclogitic rocks of Macanao type have been presented by Navarro (1974), Blackburn and Navarro (1977), Rudolph (1981), Chevalier (1987) and Bocchio et al. (1996). A sketch indicating the most prominent locations is shown in Fig. 14. No omphacite-bearing metabasic rocks have so far been found in southern Macanao. Several features stand out, especially in comparison to eclogitic rocks of the Pedro Gonzalez type. Most Macanao-type rocks are distinctly more massive and contain less white mica. Phengite can be Ba-rich (10% of interlayer cations), in keeping with the generally Ba-enriched chemistry of all metabasic rocks from Margarita, which suggests interaction with circulating fluids during the subduction process (Sorensen et al., 2005). Although barroisite dominates in La-Rinconada-type rocks, amphibole in Macanao-type eclogitic rocks is Na-rich hornblende (*s.l.*) or very Ca-rich barroisite close to the ${}^B\text{Na} = 1.5$ pfu boundary. One sample from location “J” (Fig. 14) contains winchite (Maresch et al., 1982). Omphacite compositions are often enriched in aegirine component.

Even without exact quantitative thermobarometry, the analytical and microtextural data on garnet provide valuable qualitative information on P-T conditions of metamorphism. They also provide much food for discussion. Navarro (1974, 1981) and Blackburn and Navarro (1977) first pointed out that garnets in eclogitic rocks can show complicated zoning patterns from core to rim. Figs. 15-18 show some prominent examples. Some of the patterns are smooth, while others are indicative of episodic garnet growth, of growth interruptions and even of garnet resorption. Navarro (1974, 1977, 1981, 1997) and Blackburn and Navarro (1977) have interpreted these zoning patterns as evidence for polymetamorphism and two distinct metamorphic events. Navarro (1997) most recently suggested two distinct P-T conditions of 350°C/8.5-9kbar and 600°C/11-13 kbar. The concept of two-stage polymetamorphism has had a profound influence on a number of geodynamic models of the southern Caribbean. Maresch and Abraham (1981), Beets et al. (1984), Maresch et al. (2009), and more cautiously also Chevalier (1987), have taken the position that the observed garnet zoning can be explained within a single cycle of high-pressure, low-temperature metamorphism in a subduction/collision event.

The issue is not easily resolved with the data at hand. As Blackburn and Navarro (1977) point out, there are well-documented cases of polymetamorphic garnets. On the other hand, modern petrological modeling tools have allowed a better understanding of the very complicated controlling parameters accompanying prograde garnet growth in eclogite (e.g. Hoschek, 2004; Konrad-Schmolke et al. 2007, to name just two examples). It seems relatively clear now that the garnet observed in an eclogite can have grown over a temperature interval of 100°C and more, with changing reaction partners along the way. Fractionation effects and overstepping of reaction boundaries may play an additional role. In the end, only such modeling on the basis of the effective bulk composition of each sample can provide an unequivocal answer. Age dating, either on the basis of included zircons or Nd/Sm and Lu/Hf methods, could provide a viable alternative or corroborating evidence. Konrad-Schmolke et al. (2007) have pointed out that although in detail the garnet zoning pattern in a particular eclogite will be unique, several generalities can be made. Prograde growth-zoning patterns in eclogite garnets are characterized by increasing pyrope content as well as decreasing almandine + spessartine content from core to rim. Grossular may be variable. Although there are some cyclic variations and reversals in the case of the eclogites (Fig. 15), this general trend appears to hold, especially for Pedro-Gonzalez-type eclogitic rocks. The bell-shaped decrease of Mn also suggests that the garnet zoning is in general a prograde growth feature.

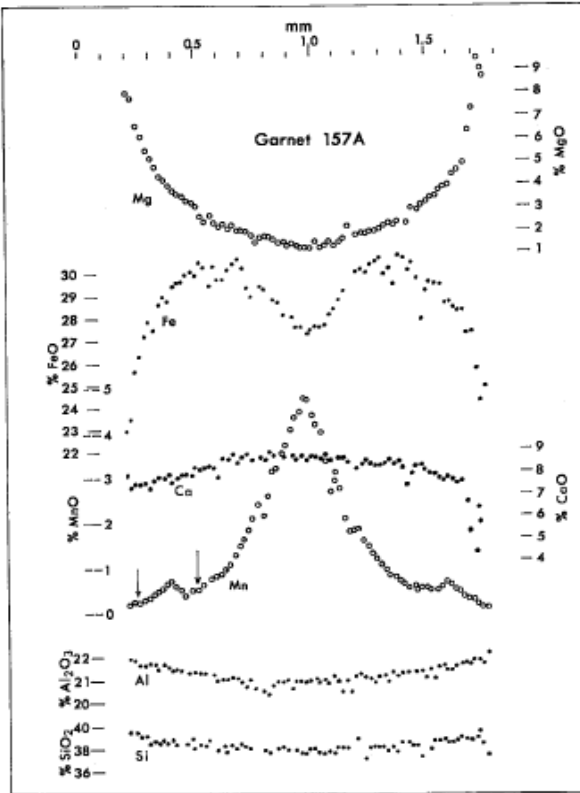


FIG. 2. Profiles of Mg, Fe, Ca, Mn, Al, and Si across garnet A from kyanite eclogite 157 (Macanao-type). Analysis points are at 20 μm intervals.

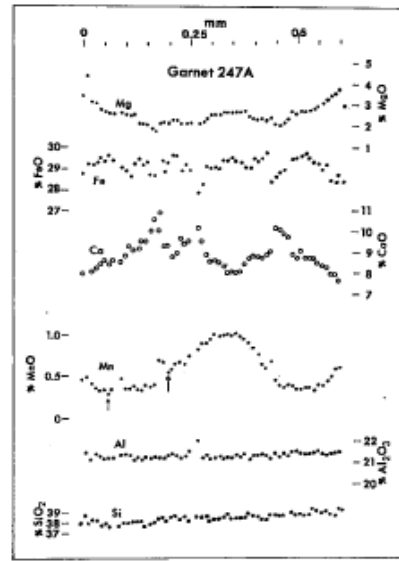


FIG. 4. Electron microprobe profile across garnet 247A. Analytical spot interval is 10 μm .

Fig. 15: Garnet profiles from Blackburn and Navarro (1977). Left: Macanao-type eclogite; right: Pedro Gonzalez type eclogite.

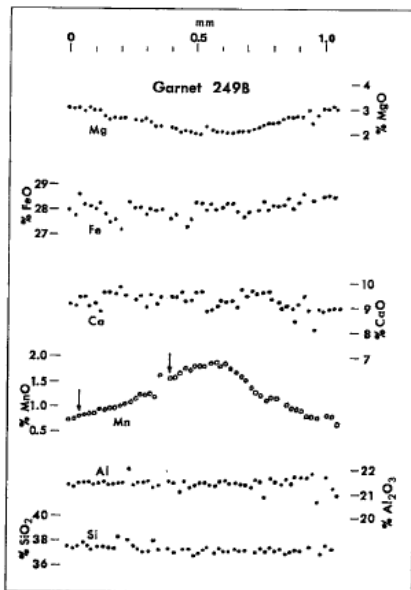


FIG. 6. Electron microprobe profile across garnet 249B. Analytical spot interval is 20 μm .

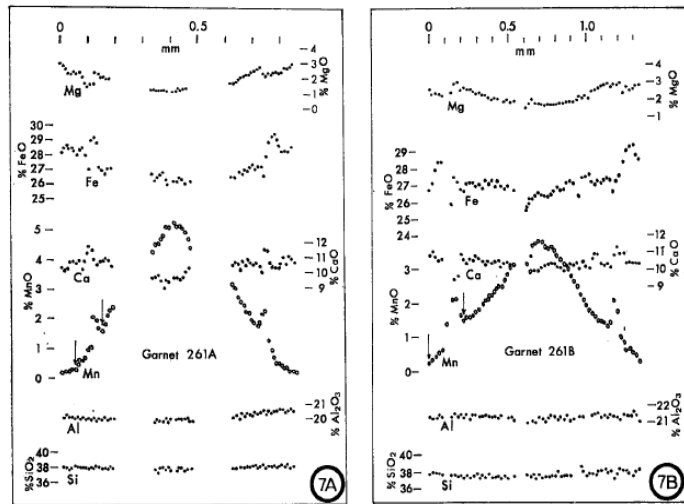


FIG. 7. (A): Microprobe profile across garnet A from amphibole eclogite 261. Step scanning at 10 μm intervals was done on three linear traverses. (B): Profile across garnet B from amphibole eclogite 261. Analytical spot interval is 20 μm .

Fig. 16: Garnet profiles from Blackburn and Navarro (1977). Amphibole eclogites.

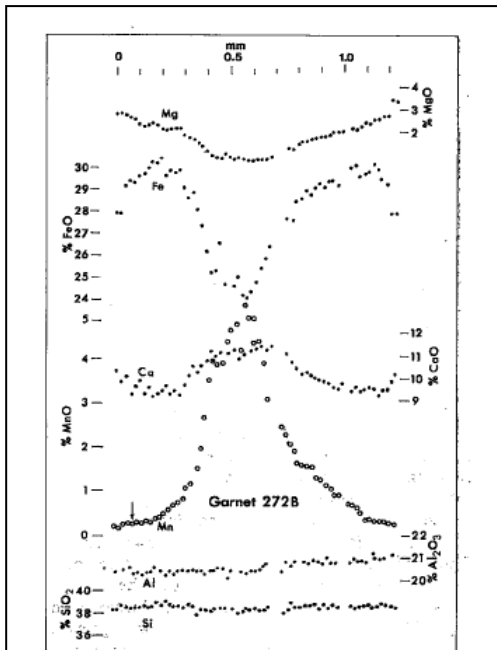


Fig. 10. Microprobe profile across garnet B from garnet amphibolite 272. Analyses are at 20 μm intervals.

Fig. 17: Garnet profiles from Blackburn and Navarro (1977). Garnet amphibolite.

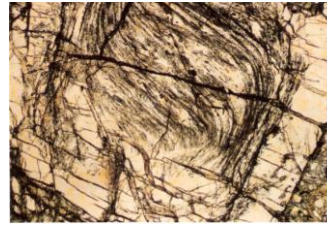


Fig. 18: Garnet crystal (~ 1 mm diameter, polarized light) from an amphibole-eclogite (Macanao type). Note the helicitic whorl and the sharp, clear overgrowth.

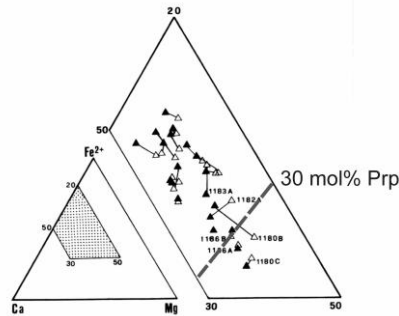


Fig. 19: Garnet compositions from Macanao - type eclogitic rocks.

As discussed by Carswell (1990), it has long been known that eclogites can be systematically differentiated on the basis of their geological occurrence (Eskola, 1921), mineral compositions (Coleman et al., 1965) or a combination of geological occurrence as well as rock and mineral composition (Smulikowski, 1964, 1968, 1972). Carswell (1990) suggested a division into low-, medium- and high-temperature eclogites, with the boundaries at 550° and 900°C, respectively. These boundaries would then coincide approximately with pyrope contents of 30 and 55 mol% pyrope in garnet solid solution. On this basis, all analyzed garnets in Pedro-Gonzalez-type rocks classify them as low-temperature eclogites. By contrast, a number of Macanao-type eclogites are of the medium-temperature type (Fig. 19), specifically from localities “G”, “K”, and “E” (Fig. 14). Of critical importance are the kyanite eclogites described by Navarro (1974, 1981) from northern Macanao (Fig. 14) and from locality “E” by Chevalier (1987). From the “pseudosections” calculated by Hoschek (2004) and Konrad-Schmolke et al. (2007) we can conclude that kyanite eclogites can only form at $T > 600^\circ\text{C}$ and pressures above 20 kbar. These results lend some credence to the determination (610-625°C/18-20 kbar) of Maresch et al. (2000) using garnet-omphacite-phengite in the internally consistent formulation of Waters and Martin (1993) for two samples from location “N” and “I” (Fig. 14), although the phengite in these rocks is very Ba-rich.

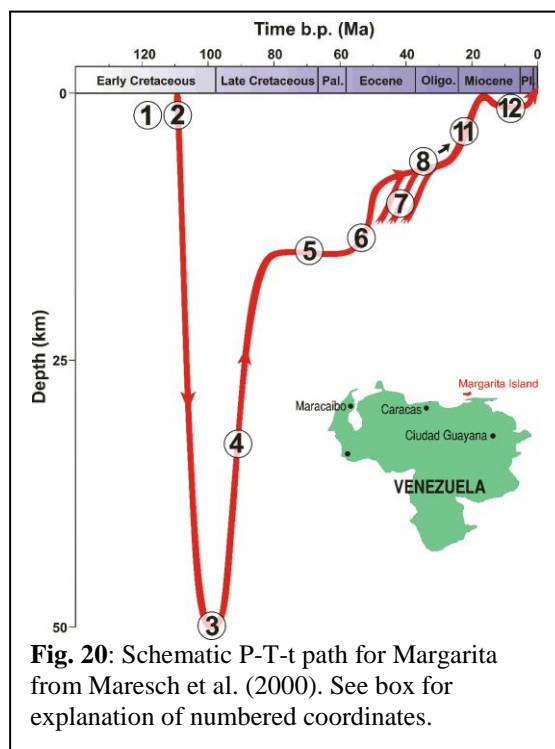
Synopsis of metamorphic field gradient:

As far as peak metamorphic conditions are concerned, the above results seem to indicate a general trend of lower pressures and temperatures in NE Margarita as compared to the rest of the island. There may also be a trend toward higher temperatures from north to south in the JGMS. However, in gauging the results of these pressure and temperature determinations on JGMS and PMC rocks in terms of regional patterns, it must be kept in mind that the present erosional level of exhumation may differ considerably across Margarita. As noted by Stöckhert et al. (1995), the late history of Margarita has been one of periods of normal and reverse faulting, leading to differential behaviour of neighbouring crustal blocks. Whereas zircon fission track data from NE Margarita cluster at ~ 50 Ma (Stöckhert et al., 1995), comparable data from Macanao can be as young as ~ 36 Ma (Brix, pers. commun.). Assuming for the sake of argument an exhumation rate

of 1mm/year, such a time difference could indicate that neighbouring crustal segments may represent erosional levels differing by as much as 10-15 kilometers.

Summary and geodynamic models

The basic data constraints for models of the geodynamic development of Margarita as expressed by Chevalier (1987), and modified by Rekowski and Rivas (2005), on the one hand, and as proposed by Stöckhert et al. (1995) and modified by Maresch et al. (2000, 2009) on the other, are summarized in Table 4 and Fig. 20, respectively.



- 1+2) Beginning of juxtaposition of oceanic (PMC) and continental (JGMS) sequences. ~110 Ma
- 3) Peak of HP/LT metamorphism between ~110 and 86 Ma.
- 4) Exhumation marked by age of non-HP-overprinted two-mica El Salado Metagranite. Cooling ages on HP phengite of JGMS.
- 5) Greenschist-facies overprint in ductile shear zones in middle crust. Progressively younger ages of recrystallizing phengite.
- 6) Exhumation into brittle regime of upper crust beginning at 55-50 Ma (youngest phengites, Rb-Sr thin-slab technique, zircon fission tracks). Basaltic dike swarms.
- 7-11) Exhumation differs in dissected blocks: variable zircon fission track data (53-36 Ma); apatite fission track data (23 Ma). Several reverse- and normal-faulting episodes.
- 12) Undisturbed Miocene sedimentation.

In terms of the geodynamic model the main differences and similarities can be seen as follows:

In order to juxtapose oceanic material (PMC) with the continental margin of South America (JGMS), Chevalier (1987) and Rekowski and Rivas (2005) call on an early Jurassic/Early Cretaceous obduction event. Evidence for this event is circumstantial. Chevalier (1987) sees some evidence for blueschists in Araya, and sees the prograding “ophiolites” as the source of gabbroic olistoliths in the continental margin sediments. Proximity of an island arc leads to deposition of volcanoclastic sediments with continental clastics as well as carbonates and black shales due to restricted circulation. These sequences then comprise the protoliths of the LRMS. HP-LT metamorphism is then due to island-arc/margin collision in the Senonian (Fig. 21). During and after the collision an intricate system of nappes is developed (Fig. 22).

However, all evidence at hand indicates that during the Jurassic-Cretaceous, northeastern South America was primarily a passive margin situation (Pindell and Kennan, 2009). Although Maresch et al. (2009) conclude, as does Chevalier (1987), that HP-LT metamorphism on Margarita Island is due to island-arc/margin collision, they call for this collision to have occurred far to the west during closure of a back-arc basin in NW Colombia. Juxtaposition of oceanic and continental margin material occurred in this subduction zone during collision without a previous obduction event. This sequence of events is summarized in Fig. 23 and 24.

Table 4: Summary taken from Rekowski and Rivas (2005).

Unidades		Metamorfismo / Protolito	Observaciones/ Edad
Diques máficos		P: ígneo M: no presenta, sólo leve alteración hidrotermal	Intrusionados en un régimen de deformación frágil, en un alto nivel de la corteza / Eoceno medio
Volcánicas de Los Frailes		P: ígneo volcánico y sedimentario M: no presenta	Magmatismo Cretácico y emplazamiento como olistolito en el Eoceno / Maastrichtiense
Rocas Metagraníticas	Pegmatitas	P: ígneo M: no presenta, sólo fueron afectadas por plegamiento durante la tercera fase de deformación y por leve alteración hidrotermal	Última manifestación de magmatismo ácido / Paleoceno – Eoceno temprano
	Metagranito de San Juan Bautista	P: ígneo plutónico M: baja P/T	Intrusión de afinidad calco-alkalina *
	Metagranodiorita de Agua de Vaca	P: ígneo plutónico (¿carácter intermedio continental con transición oceánica?)* M: baja P/T. Facies de los esquistos verdes.*	
	Metagranito de El Salado	P: ígneo plutónico (calco-alkalina, arco relacionada) M: baja P/T. Facies de los esquistos verdes.	
	Metatromdjemita de Matasiete	P: ígneo plutónico (magmatismo oceánico) M: alta P/T y luego de baja P/T	Intrusiones plutónicas de afinidad calco-alkalina, que afectan al bloque ofiolítico/114-105 Ma (Aptiense – albiense). Probables plagiogranitos.
	Gneis de Guayacán		

Unidades		Metamorfismo / Protolito	Observaciones/ Edad
Asociación Metamórfica Los Robles		P: sedimentario M: baja P/T. Facies de los esquistos verdes.	Cobertura sedimentaria del Complejo Metaofiolítico Paraguachí, puesta en contacto con las secuencias anteriores después del evento de acreción / Cretácico
Complejo Metaofiolítico Paraguachí	Metavolcánicas de Manzanillo	P: ígneo volcánico M: Intermedia P/T. Facies de los esquistos verdes	Litosfera oceánica obducida sobre el paleomargen Suramericano / Jurásico – Cretácico?
	Metamáficas de La Rinconada	P: ígneo – Basalto tipo MORB M: eventos sucesivos de alta P/T 1º: Facies de los esquistos azules 2º: Facies de la eclogita y de la anfíbolita epidótica	
	Metaultramáficas de Cerro El Copey	P: ígneo plutónico (corteza oceánica o manto) M: Intermedia P/T. Facies de los esquistos verdes.	
Asociación Metamórfica Juan Griego		P: ígneo (corteza continental) – sedimentario (sedimentos pelíticos y carbonáticos) M: Variable. Facies de la Anfíbolita epidótica a facies de los esquistos verdes.	Serie de paleomargen (corteza continental del Jurásico con elementos de basamento Paleozoico) / Pensilvaniense – Cretácico?

Abreviaturas P: protolito, M: metamorfismo * Datos inciertos

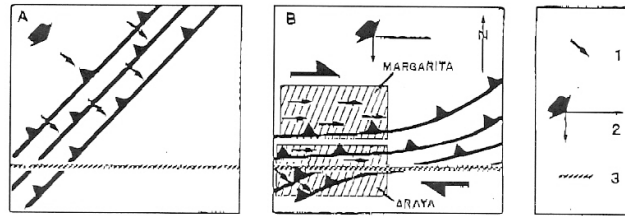
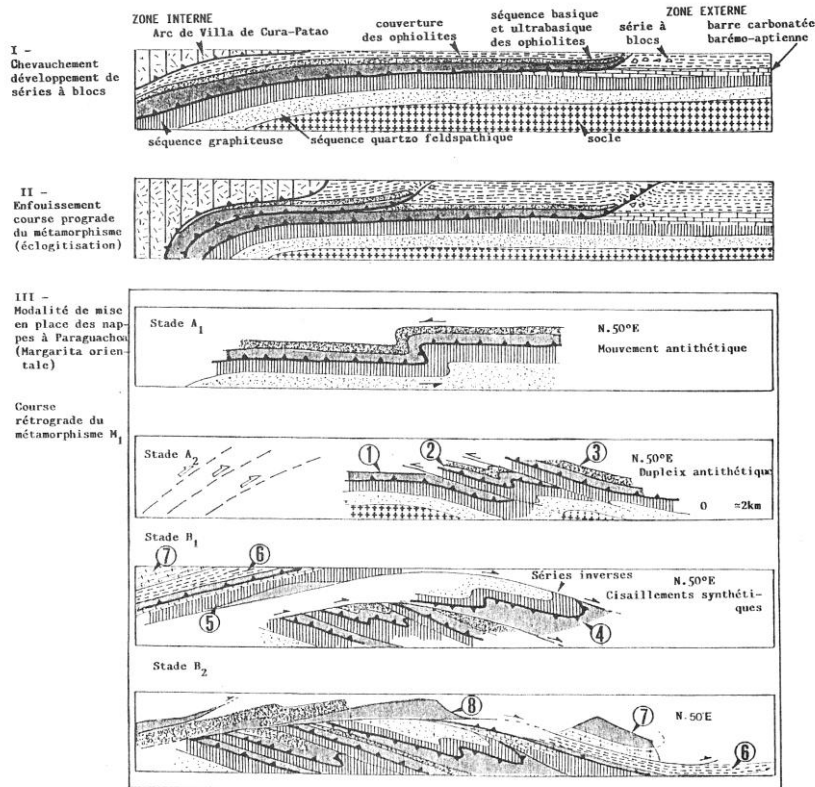


Fig. 3

Fig. 3. — Interprétation cinématique des structures majeures synmétamorphes D1-S1. (A) stade initial : plis et chevauchements naissent dans une direction perpendiculaire à celle du vecteur de convergence; la linéation d'allongement L1 (1) est parallèle à ce dernier. (B) stade évolué : la direction de convergence se décompose en deux vecteurs (2), l'un parallèle, l'autre perpendiculaire à une discontinuité crustale (3) de la paléomarge américaine; au niveau de Margarita la linéation d'allongement L1 se réoriente parallèlement à cette discontinuité.

Fig. 3. — Kinematic interpretation of D1-S1 synmetamorphic major structures. (A) Initial stage: folds axis and thrust fronts appear perpendicularly to the convergence direction; the stretching lineation L1 (1) is parallel to that one. (B) Evolved stage: the convergence direction splits itself into two vectors (2), one parallel, the other perpendicular to a crustal discontinuity (3) in the South America paleomargin. On Margarita, the stretching lineation reorientated itself parallel to that discontinuity.

Fig. 21: Collision of island arc with South American margin containing obducted ophiolites. Taken from Chevalier et al. (1988).



Légende des différentes nappes:

1. Nappe de Santa Ana
2. Nappe de La Rinconada
3. Nappe de El Salado
4. Nappe d'El Chorro - La Asuncion
5. Nappe d'El Fiacho
6. Nappe de Los Robles
7. Nappe du Matasieste Guayamuri
8. Nappe du Cerro Chico - Pedro Gonzalez

Fig. 169 - Schémas illustrant les modalités envisagées pour la mise en place des nappes de l'Ensemble supérieur de Paraguachoa (Margarita orientale)

Esquemas ilustrando las modalidades previstas para el emplazamiento de las unidades aloctonas en la península de Paraguachoa (Margarita oriental)

Fig. 22: Nappe development during collision shown in Fig. 21. Taken from Chevalier (1987).

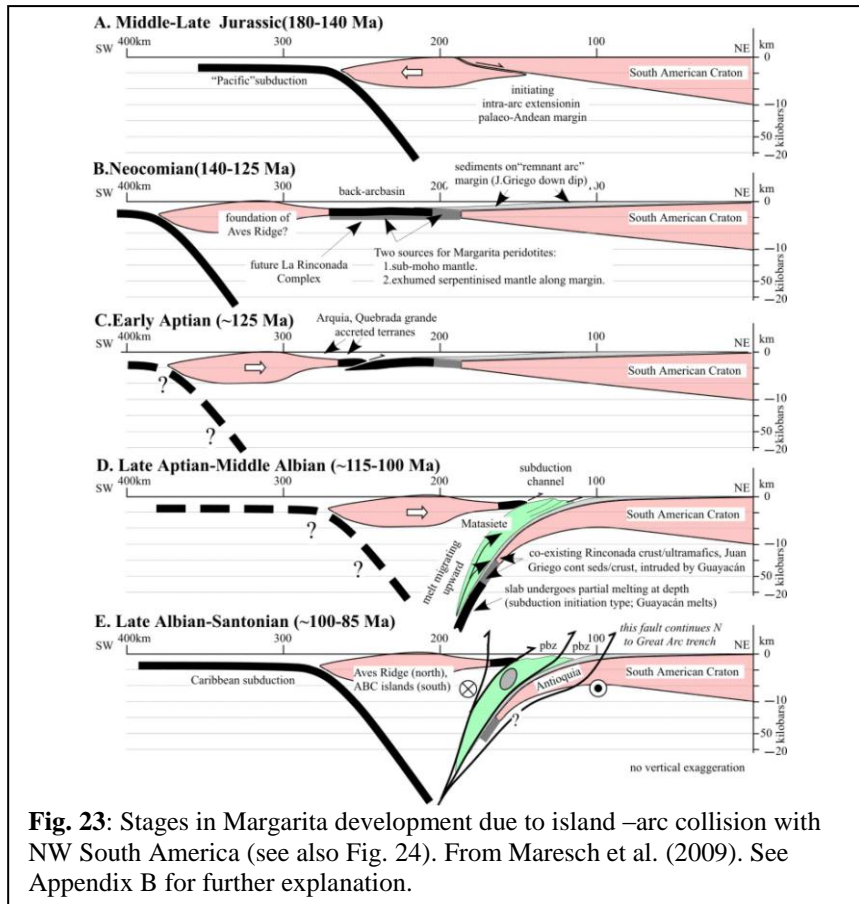


Fig. 23: Stages in Margarita development due to island-arc collision with NW South America (see also Fig. 24). From Maresch et al. (2009). See Appendix B for further explanation.

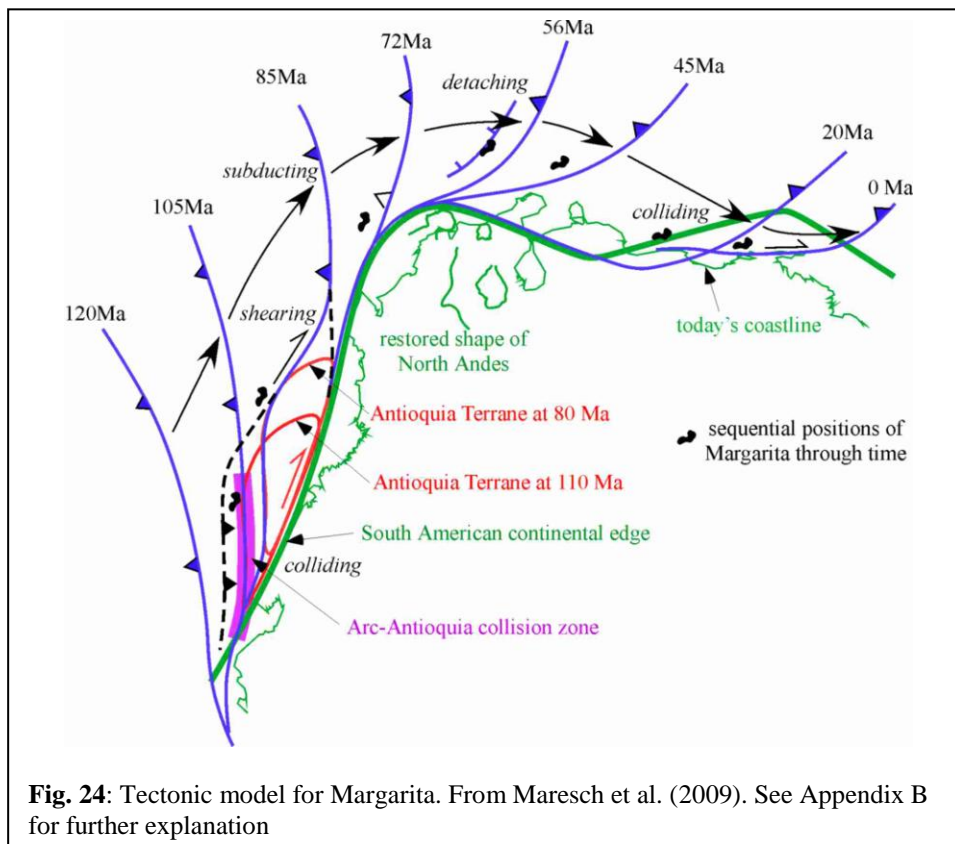


Fig. 24: Tectonic model for Margarita. From Maresch et al. (2009). See Appendix B for further explanation

With the exception of the development of the intricate nappe structure described by Chevalier (1987) and Rekowski and Rivas (2005), the ductile exhumation path proposed in both scenarios is quite similar (Fig. 8, 20), with the age data given in Stöckhert et al. (1995) and Maresch et al. (2000, 2009) providing narrow constraints on timing. Chevalier (1987) already noted that “deracinated” JGMS, i.e. uprooted parts of the overridden continental margin, were involved in high-pressure metamorphism and nappe development of the PMC. Maresch et al. (2009) conclude that ALL of the JGMS is “deracinated” continental margin derived from NW South America. The major overthrust between relative autochthon and PMC-dominated nappes postulated by Chevalier (1987) and others (e.g., Higgs, 2009) is not required, and, in the opinion of Maresch et al. (2009), there is no evidence for such a major discontinuity between JGMS and PMC on Margarita.

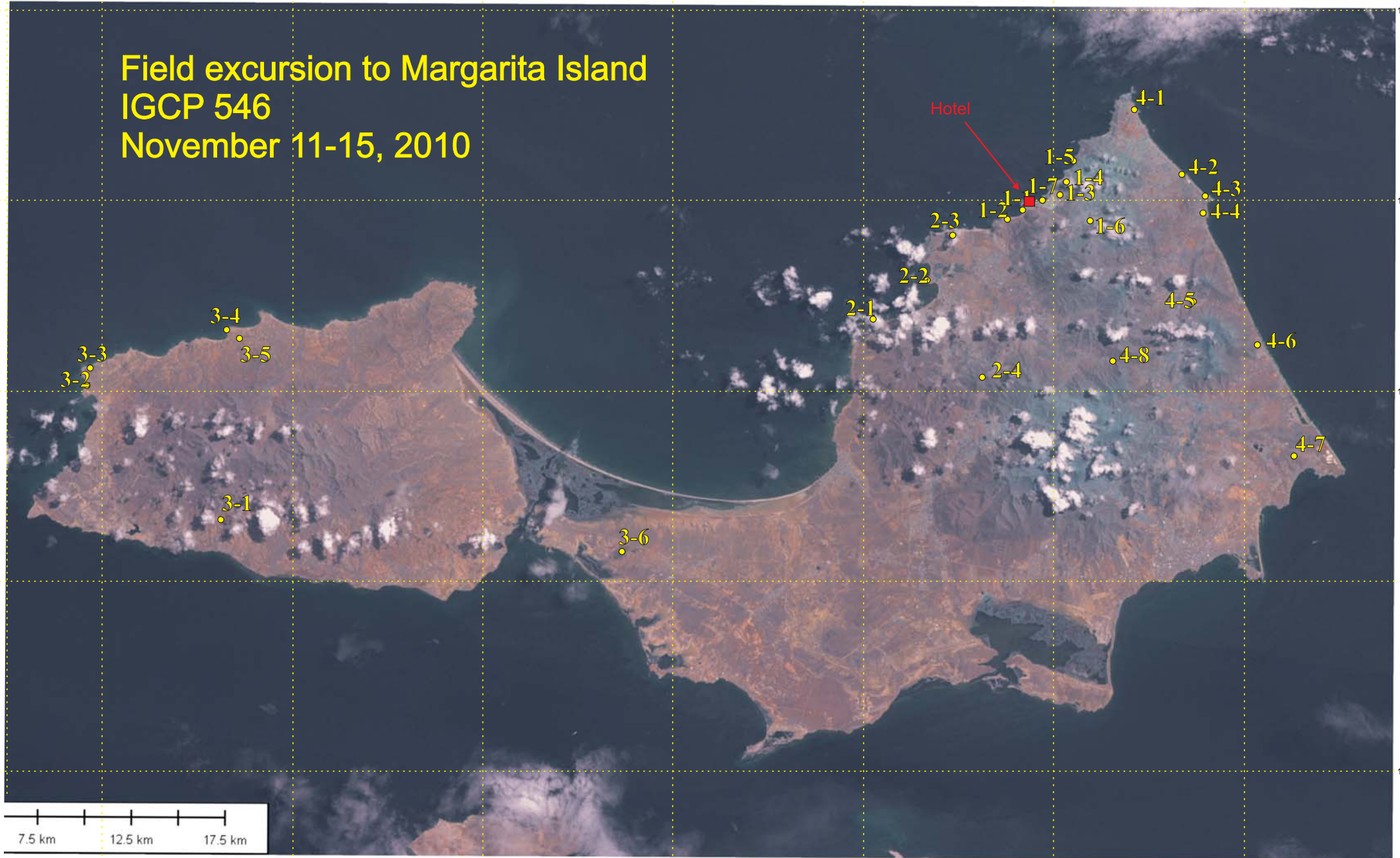
References cited

- Avé Lallemant, H. G. (1997) Transpression, displacement partitioning, and exhumation in the eastern Caribbean/South American plate boundary zone. *Tectonics*, **16**, 272-289.
- Beets DJ, Maresch WV, Klaver G., Mottana A, Bocchio R, Beunk FF, Monen HP (1984) Magmatic rock series and high-pressure metamorphism as constraints on the tectonic history of the southern Caribbean. *Geol. Soc. America Memoir*, **162**, 95-130.
- Beysac O., Goffé B., Chopin C., Rouzaud J.N. (2002) Raman spectra of carbonaceous material in metasediments: a new geothermometer. *J. metamorphic Geol.*, **20**, 859-871.
- Blackburn W, Navarro F., E (1977) Garnet zoning and polymetamorphism in the eclogitic rocks of isla de Margarita, Venezuela. *Can. Mineralogist*, **15**, 257-266.
- Bocchio R, De Capitani L, Liborio G, Maresch WV, Mottana A (1990) The eclogite-bearing series of Isla Margarita, Venezuela: Geochemistry of metabasic lithologies in the La Rinconada and Juan Griego Groups. *Lithos*, **25**, 55-69.
- Bocchio R, De Capitani L, Liborio G, Maresch WV, Mottana A (1996) Equilibration conditions of eclogite lenses from Isla Margarita, Venezuela: Implications for the tectonic evolution of the metasedimentary Juan Griego Group. *Lithos*, **37**, 39-59.
- Carswell DA, ed. (1990) *Eclogite Facies Rocks*. Blackie, 396 pp.
- Carswell DA (1990) Eclogites and the eclogite facies: definitions and classification. In: Carswell DA, ed. *Eclogite Facies Rocks*. Blackie, 1-13.
- Chevalier Y (1987) *Les zones internes de la chaîne sud-caraïbe sur la transect: Ile de Margarita – Péninsula d'Araya (Venezuela)*. PhD thesis, Université de Bretagne Occidentale, Brest, France, 504 pp.
- Chevalier Y, Stephan J-F, Darboux J-R, Gravelle M, Bellon H, Bellizzia A, Blanchet R (1988) Obduction et collision pré-Tertiaire dans les zones internes de la Chaîne Caraïbe vénézuélienne, sur le transect Ile de Margarita-Péninsule de Araya. *Comptes rendues de la Academie des Sciences Paris*, **307**(II), 1925-1932.
- Coleman RG, Lee DE, Beatty LB, Brannock WW (1965) Eclogites and eclogites: their differences and similarities. *Geol. Soc. America Bull.*, **76**, 483-508.
- Giunta G, Beccaluva L, Coltorti M, Siena F, Vaccaro C (2002) The southern margin of the Caribbean Plate in Venezuela: tectono-magmatic setting of the ophiolitic units and kinematic evolution. *Lithos*, **63**, 19-40.
- González de Juana C, Vignali M (1972) Rocas metamórficas e ígneas en la península de Macanao, Margarita, Venezuela, Venezuela. Mem. VI Conf. Geol. del Caribe, 1971, 63-68.
- Guth LR, Avé Lallemant HG (1991) A kinematic history for eastern Margarita Island, Venezuela. In: Larue, D.K., and Draper, G. (eds) *Transactions 12th Caribbean Geological Conference, 1989, St. Croix, Miami Geological Society*, 472-480.
- Higgs R (2009) Caribbean-South America oblique collision model revised. In: James, K., Lorente, M.A., and Pindell, J.L. (eds) *The Origin and Evolution of the Caribbean Plate*, Geological Society of London, Special Publications, **328**, 613-657.
- Hoschek G (2004) Comparison of calculated *P-T* pseudosections for a kyanite eclogite from the Tauern Window, Eastern Alps, Austria. *Eur. J. Mineral.*, **16**, 59-72.
- James KH, Lorente MA, Pindell J (eds) (2009) *The geology and evolution of the region between North and South America*, Geological Society of London, Special Publications, **328**, 858 pp.
- Kaiser C (1996) *Multi-component evolution, age and plate-tectonic setting of high-Mg lamprophyric dikes and gabbros on Isla Margarita (Venezuela)*. PhD thesis, Ruhr-University Bochum, Bochum, Germany, 188+50 pp.
- Kluge R (1996) *Geochronologische Entwicklung des Margarita-Krustenblocks, NE Venezuela*. PhD Thesis, University of Münster, Münster, Germany, 196 pp.
- Konrad-Schmolke M, O'Brien P, de Capitani C, Carwell DA (2007) Garnet growth at high- and ultra-high pressure conditions and the effect of element fractionation on mineral modes and composition. *Lithos*, doi:10.1016/j.lithos.2007.10.1007.

- Konzett J, Hoinkes G (1996) Paragonite-hornblende assemblages and their petrological significance: an example from the Austroalpine Schneeberg Complex, Southern Tyrol, Italy. *J. metam. Geol.*, **14**, 85-101.
- Kramm U (1976) The coticule rocks (spessartine quartzites) of the Venn Stavelot Massif, Ardennes, a volcanoclastic metasediment? *Contr. Min. Petr.*, **56**, 135-155.
- Krosse S, Schreyer (1993) Comparative geochemistry of coticules (spessartine quartzites) and their redschist country rocks in the Ordovician of the Ardennes Mountains, Belgium. *Chem. Erde*, **53**, 1-20.
- Krückhans-Lueder, GE (1996) *Petrologie und Geochemie der Juan-Griego-Einheit, Insel Margarita (Venezuela)*. PhD Thesis, University of Münster, Münster, Germany, 285 pp.
- Lázaro C, García-Casco A (2008) Geochemical and Sr-Nd isotope signatures of pristine slab melts and their residues (Sierra del Convento mélange, eastern Cuba). *Chemical Geology*, **255**, 120-133.
- Macsoyay O, Chachati B, Avarez . (1997) Eventos de sedimentación, intrusión y sobrecorrimiento en Macanao, Estado Nueva Esparta, Venezuela nor-oriental. *Memorias del VIII Congreso Geológico Venezolano*, **11**, 17-24.
- Maresch WV (1971) *The metamorphism of northeastern Margarita Island, Venezuela*. Ph.D. thesis, Princeton University, USA, 278 pp.
- Maresch WV (1973) Metamorfismo y estructura de Margarita Oriental, Venezuela. *Boletín Geológico del Ministerio de Minas e Hidrocarburos*, **XII/22**, 3-172.
- Maresch WV (1975) The geology of northeastern Margarita Island, Venezuela: A contribution to the study of Caribbean plate margins. *Geologische Rundschau*, **64**, 846-883.
- Maresch WV (1977) Similarity of metamorphic gradients in time and space during metamorphism of the La Rinconada Group, Margarita Island, Venezuela. *G.U.A. Papers in Geology, Amsterdam*, **1**, 110-111.
- Maresch WV, Abraham K (1977) Chemographic analysis of reaction textures in an eclogite from the Island of Margarita (Venezuela). *N. Jb. Miner. Abh.*, **130**, 103-113.
- Maresch WV, Abraham K (1981) Petrography, mineralogy and metamorphic evolution of an eclogite from the Island of Margarita, Venezuela. *Journal Petrology*, **22**, 337-362.
- Maresch WV, Medenbach O, Rudolph A (1982) Winchite and the actinolite-glaucophane miscibility gap. *Nature*, **296**, 731-732.
- Maresch WV, Stöckert B, Baumann A, Kaiser C, Kluge R, Krückhans-Lueder G, Brix MR, Thomson S (2000) Crustal history and plate development in the southern Caribbean. *Zeitschr. Ang. Geologie*, **SH1**, 283-289.
- Maresch WV (1975) The geology of northeastern Margarita Island, Venezuela: A contribution to the study of Caribbean plate margins. *Geologische Rundschau*, **64**, 846-883.
- Maresch WV, Stöckert B, Baumann A, Kaiser C, Kluge R, Krückhans-Lueder G, Brix M, Thomson S (2000) Crustal history and plate tectonic development in the southeastern Caribbean. *Z. Angew. Geol.*, **SH1**, 283-290.
- Maresch WV, Kluge R, Baumann A, Pindell J, Krückhans-Lueder G, Stanek KP (2009) The occurrence and timing of high-pressure metamorphism on Margarita Island, Venezuela: a constraint on Caribbean –South America interaction. In: James, K.H., Lorente M.A. & Pindell, J.L. (eds) *The Origin and Evolution of the Caribbean Plate*, Geological Society of London Special Publication, **328**, 705-741.
- Molina JF, Poli S (1998) Singular equilibria in paragonite blueschists, amphibolites and eclogites. *J. Petrology*, **39**, 1325-1346.
- Mottana A, Bocchio R, Liborio G, Morten L, Maresch WV (1985) The eclogite-bearing metabasaltic sequence of Isla Margarita, Venezuela: A geochemical study. *Chemical Geology*, **50**, 351-368.
- NACSN – North American Commission on Stratigraphic Nomenclature. 1983. North American Stratigraphic Code. *AAPG Bull.* 67(5): 841-875.
- NACSN – North American Commission on Stratigraphic Nomenclature. 2005. North American Stratigraphic Code. *AAPG Bull.* 89(11): 1547-1591.
- Navarro F., E (1974) Petrogenesis of the eclogitic rocks of isla de Margarita, Venezuela. Ph.D. Diss., University of Kentucky, 213 pp.
- Navarro E (1987) Trondhjemitas de Matasiete, Estado Nueva Esparta: Un plagiogranito Océanico. *Mem. I^{as} Jor. Invest. Ing.*, 110-113.
- Navarro F, E (1997) Granate-clinopiroxeno-fengita. Geotermometría y barometría en las eclogitas de la isla de Margarita. *Mem. VIII Congr. Geol. Venezolano*, 195-201.
- Navarro F., E (1977) Eclogitas de Margarita. Evidencias de polimetamorfismo. *Mem. V Congr. Geol. Venezolano*, 651-661.
- Navarro F., E (1981) Relaciones mineralógicas en las rocas eclogíticas de la isla de Margarita, Estado Nueva Esparta. *Geos*, **26**, 3-44.
- Navarro F., E, Ostos R., M (1997) Algunas consideraciones sobre el ambiente tectónico de origen de las leucotonalitas de la isla de Margarita. *Mem. VIII Congr. Geol. Venezolano*, 203-209.
- Newton RC (1986) Metamorphic temperatures and pressures of Group B and Group C eclogites. In: Evans BW, Brown BH (eds) *Blueschists and Eclogites*. Geol. Soc. America Mem., 164, 17-30.
- Ostos M, Sisson VB (2005) Geochemistry and tectonic setting of igneous and metaigneous rocks of northern Venezuela. In: James, K.H., Lorente M.A. & Pindell, J.L. (eds) *The Origin and Evolution of the Caribbean Plate*, Geological Society of London Special Publication, **328**, 119-156.

- Pindell JL, Kennan L (2009) Tectonic evolution of the Gulf of Mexico, Caribbean and northern South America in the mantle reference frame: an update. In: James, K.H., Lorente, M.A., and Pindell, J.L. (eds) *The Origin and Evolution of the Caribbean Plate*, Geological Society of London, Special Publications, **328**, 1-55.
- Rekowski F, Rivas L. (2005) Integración geológica de la isla de Margarita, estado Nueva Esparta. *Geos*, UCV, Caracas, **38**: 97-98 (+ 242 p. and 18 maps in CD).
- Rudolph A (1981) *Petrographie und Petrologie von eklogitischen Linsen in Glimmerschiefern der Insel Margarita, Venezuela*. MSc thesis, Ruhr-University Bochum, Bochum, Germany, 93+44 pp.
- Scherer W. (ed.) 1997. *Código Estratigráfico de las Cuencas Petroleras de Venezuela*. <http://www.pdvsa.com/lexico/lexicoh.htm>
- Schliestedt M (1980) *Phasengleichgewichte in Hochdruckgesteinen von Sifnos, Griechenland*. Ph.D. Diss., University of Braunschweig, Germany, 142 pp.
- Selverstone J, Franz G, Thomas S, Getty S (1992) Fluid variability in 2 GPa eclogites as an indicator of fluid behaviour during subduction. *Contr. Min. Petrol.*, **112**, 341-357.
- Smulikowski K (1964) An attempt at eclogite classification. *Bull. de l'Acad. Polonaise Sciences*, **12**, 27-33.
- Smulikowski K (1968) Differentiation of eclogites and possible causes. *Lithos*, **1**, 89-101.
- Smulikowski K (1972) Classification of eclogites and allied rocks. *Krystallinikum*, **9**, 107-130.
- Sorensen SS, Sisson VB, Avé Lallemand HG (2005) Geochemical evidence for possible trench provenance and fluid-rock histories, Cordillera de la Costa eclogite belt, Venezuela. In: Avé Lallemand HG, Sisson VB (eds) *Caribbean-South American Plate Interactions, Venezuela*. Geological Society of America Special Paper, **394**, 173-192.
- Stöckhert B, Maresch WV, Toetz A, Kluge R, Krückhans G, Kaiser C, Aguilar V, Klier T, Laupenmühlen S, Piepenbreier D, Wiethe I (1993) Tectonic history of Isla Margarita, Venezuela – a record of a piece of crust close to an active plate margin. *Zentralblatt für Geologie und Paläontologie*, **Heft 1993**, 485-498.
- Stöckhert B, Maresch WV, Brix M, Kaiser C, Toetz A, Kluge R, Krückhans-Lueder G (1995) Crustal history of Margarita Island (Venezuela) in detail: constraint on the Caribbean plate-tectonic scenario. *Geology*, **23**, 787-790.
- Taylor G. C. 1960. Geología de la Isla de Margarita. *Mem. III Cong. Geol. Venezolano*, Caracas, 1959. *Bol. Geol.*, MMH, Caracas, *Pub. Esp.* 3, 2: 838-893.
- Urbani F (2007) Las regiones de rocas ígneas y metamórficas del norte de Venezuela. *Mem. IX Congr. Geol. Venezolano*, 21-25; *Geos*, Caracas, **39**, 93 + 11 p. in CD.
- Urbani F. 2008. Revisión de la nomenclatura de las unidades de rocas ígneas y metamórficas del norte de Venezuela. *Bol. Acad. Cienc. Fís., Mat. Nat.*, Caracas, 68(3): 27-44
- Waters DJ, Martin HN (1993) Geobarometry in phengite-bearing eclogites. *Terra Abstracts*, **5**, 410-411.
- Willner AP, Pawlig S, Massonne HJ, Hervé F (2001) Metamorphic evolution of spessartine quartzites (coticles) in the high-pressure, low-temperature complex at Bahia Mansa, Coastal Cordillera of South-Central Chile. *Can. Mineral.*, **39**, 1547-1569.

Field excursion to Margarita Island
IGCP 546
November 11-15, 2010



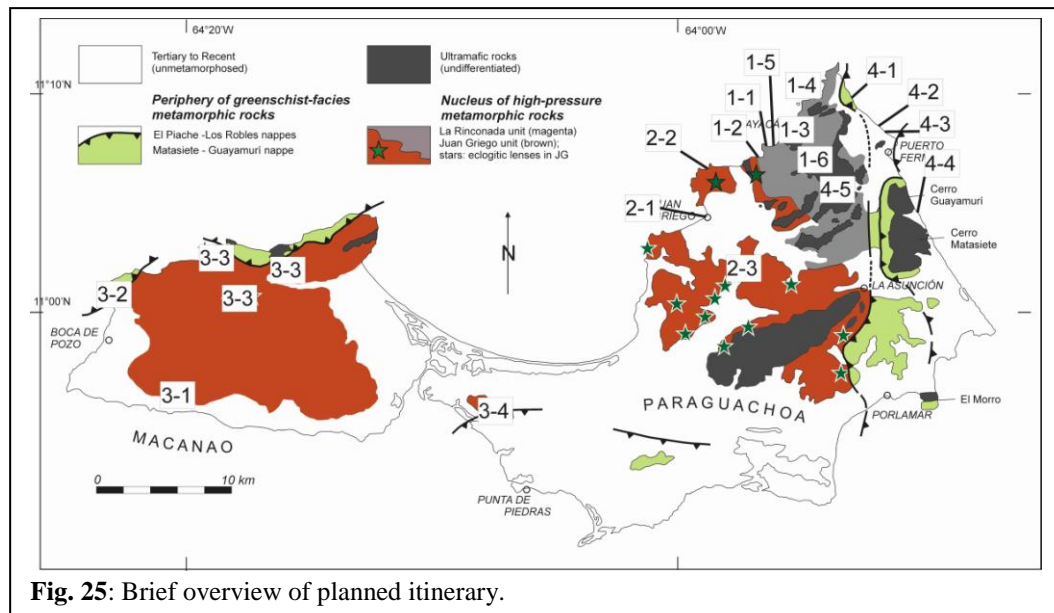
Stops of the field excursion Margarita Island 2010

Stop	date	Latitude	Longitude	locality
Stop 1-1	11. Nov 10	N11°07'16,47"	W063°55'56,56"	Playa Zaragoza, La Rinconada metabasic rocks
Stop 1-2	11. Nov 10	N11°07'03,02"	W063°56'17,65"	Playa Zaragoza, La Rinconada metabasic rocks
Stop 1-3	11. Nov 10	N11°07'40,68"	W063°54'45,41"	highway Pedro Gonzales to Manzanillo / magnesite
Stop 1-4	11. Nov 10	N11°08'03,11"	W063°54'35,52"	highway Pedro Gonzales to Manzanillo / eclogite / Guayacan gneiss
Stop 1-5	11. Nov 10	N11°08'39,41"	W063°54'23,86"	Punta Ausente
Stop 1-6	11. Nov 10	N11°06'57,57"	W063°53'52,63"	Pedro Gonzales, garnet amphibolite
Stop 1-7	11. Nov 10	N11°07'38,48"	W063°55'22,29"	beach outcrop east of the Dunes hotel
Stop 2-1	12. Nov 10	N11°04'08,28"	W064°00'08,19"	Punta Taguantar, metaconglomerate
Stop 2-2	12. Nov 10	N11°05'14,44"	W063°58'36,43"	Fortin La Galera
Stop 2-3	12. Nov 10	N11°06'31,74"	W063°57'51,29"	Playa Caribe
Stop 2-4	12. Nov 10	N11°02'18,20"	W063°57'02,68"	El Maco
Stop 3-1	13. Nov 10	N10°58'18,61"	W064°18'53,34"	El Manglillo
Stop 3-2	13. Nov 10	N11°02'13,47"	W064°22'52,80"	Robledal, metadacite
Stop 3-3	13. Nov 10	N11°02'37,75"	W064°22'45,14"	Bajo Los Oros, metagabro/Basalt dikes
Stop 3-4	13. Nov 10	N11°03'42,73"	W064°18'48,16"	La Pared, eclogite boudins
Stop 3-5	13. Nov 10	N11°03'31,59"	W064°18'27,38"	La Pared, kyanite eclogite
Stop 3-6	13. Nov 10	N10°57'27,53"	W064°07'22,51"	Las Tetas de Maria Guevara
Stop 4-1	14. Nov 10	N11°10'06,32"	W063°52'37,22"	Punta Varadero, Manzanillo unit - gabbro
Stop 4-2	14. Nov 10	N11°08'17,04"	W063°51'15,69"	Punta Cabo Blanco, diorite - gabbro dikes
Stop 4-3	14. Nov 10	N11°07'39,78"	W063°50'35,30"	Playa Parguito, Matasiete mylonite
Stop 4-4	14. Nov 10	N11°07'11,02"	W063°50'39,64"	El Tirano, Matasiete trondhjemite, less deformed
Stop 4-5	14. Nov 10	N11°04'38,49"	W063°50'56,17"	Flandes, Matasiete trondhjemite, undeformed
Stop 4-6	14. Nov 10	N11°03'25,48"	W063°49'04,34"	Guarame, harzburgite
Stop 4-7	14. Nov 10	N11°00'14,95"	W063°47'58,34"	Pampatar, flysch
Stop 4-8	14. Nov 10	N11°02'57,28"	W063°53'12,71"	El Portachuelo, La Rinconada metabasic rocks

Field excursion to Margarita Island
IGCP 546
November 11-15, 2010



Proposed Itinerary



Day 1:

Stop 1-1: Zaragoza Harbour or waterfront of Dunes Beach (depending on accessibility for non-residents of Dunes Beach hotel):

The locality unfortunately has various names on various maps (Playa Pedro Gonzalez; Punta Zaragoza; La Vela, Guayacán, etc.). If we follow the low cliffs along the NE side of the bay, i.e. along the cliffs to the west of the lighthouse, we will see a striking sequence of eclogite-facies metabasites with distinct compositional layering. For the most part these are coarse-grained rocks in which red garnet, laths of green omphacite, and porphyroblasts of white mica (paragonite, phengite, or both) are clearly visible, all set in a dark bluish-green matrix composed of barroisite amphibole and Fe-poor epidote minerals, usually clinozoisite. The latter may be concentrated into segregations of epidosite with a typical tan (rather than green!) colour. Rutile is a typical accessory and may be found as idiomorphic crystals in quartz segregations running through the rock. Some of the best examples of these rocks and the folding affecting them are found in the wave-worn boulders lining the shore of the Dunes Beach hotel east of the lighthouse promontory (Frontispiece, Fig. 26). The darker layers are essentially greenish amphibole (probably Al-poor), and often boudinaged. The lighter coloured, gneissic layers owe their colour to quartz and albite enrichment. Albite often occurs as secondary amoeboid porphyroblasts (Fig. 26, g,h).

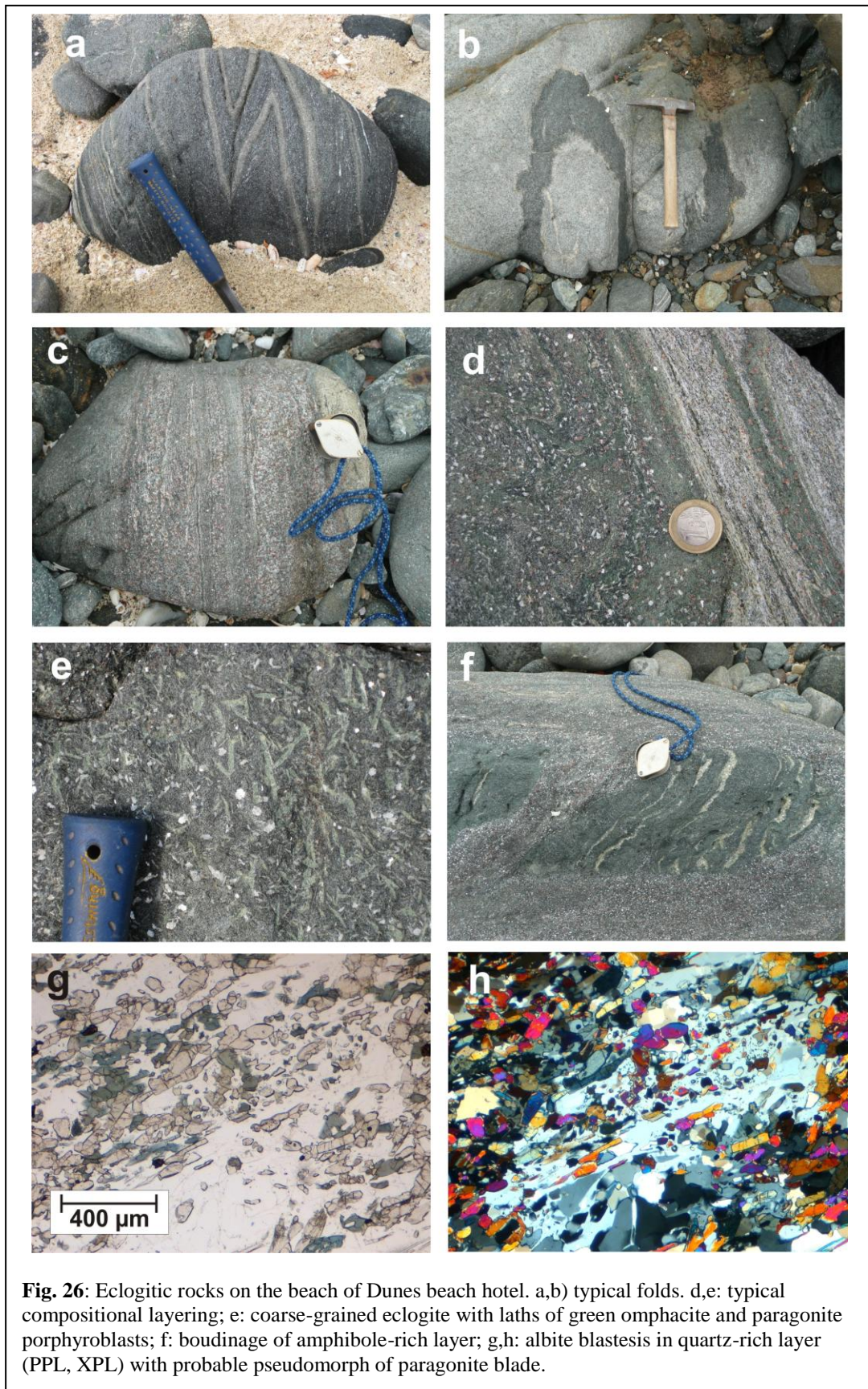
Stop 1-2: West end of La Vela beach (800 m from Stop 1):

These cliffs show typical examples of coarse-grained dark metabasic rocks of metamorphic zone II with abundant white mica and only very rare omphacite.

Stop 1-3: Walk from Hotel Isla Bonita to the Guayacán junction along north-coast road:

From La Vela beach we will drive via Pedro González to the foot of the hills rising to the northeast. This is the beginning of a lovely road that will wind along the north coast to Manzanillo. The hotel to the left was built almost directly on the outcrop of eclogite described in detail by Maresch and Abraham (1977, 1981). A whole hill was moved into the valley to the SE, where the bulldozers have now exposed a large outcrop of flaser gabbro (restricted entrance). This rock is found in many parts of the La Rinconada unit and seems to represent a fairly late type of intrusion into the metabasic series. A greenschist-facies mineralogy is typical, but

sometimes barroisite with cores of brownish hornblende may be present. The light-coloured



layers are mainly albite+clinozoisite and the green layers chlorite+actinolite. At the first road-cut we will see a very interesting and common feature for Margarita, namely the formation of gel magnesite (white veins) in altered serpentinite. Magnesite has been mined on Margarita at various times for the last 150 years. The most prominent workings are located at Cerro

Tragaplata (also called Loma de Guerra) on the east coast, but there is not much more to see there than you can observe here.

Along the road we will see typical, coarse-grained La Rinconada metabasites with omphacite- (light-green laths) and white-mica-rich (commonly paragonite, but also phengite) layers. Note again that tight folding is common and that omphacite overgrows the hinges of these folds. Look back to the SW towards stop 1-1 La Vela. Note the sand dune climbing up the back side of the cliff near the Dunes Beach hotel.

After the bend in the road we will be encountering the first light-coloured examples of Guayacán Gneiss, whose origin will be a point of discussion. On the basis of tonalitic composition and zircons with a magmatic habit, it is clearly a former magmatic rock. If we are lucky, we may still see the remnants of a landslide in 2009, where blocks of metabasite with small intrusive bodies were exposed. If not, we can turn to photographs made then (Fig. 27). Note, however, that we will see totally different contact relationships at stop 1-6 later in the day.



Fig. 27: Guayacán/metabasite intrusive relationship. 2009 landslide north- coast road.

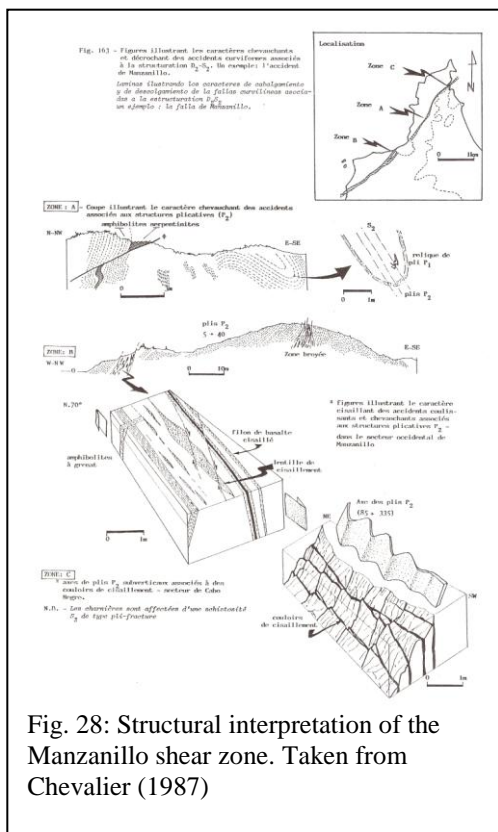


Fig. 28: Structural interpretation of the Manzanillo shear zone. Taken from Chevalier (1987)

However, is Guayacan Orthogneiss a "metaplagiogrinite" of MOR origin, thus dating the basalts of the La Rinconada Group at 116-106 Ma? Or is it the adakitic product of anatexis of subducting oceanic crust? The gneiss is now an albite+quartz+white-mica(phengite±paragonite) rock. The green laths visible in some places are barroisite amphibole (now extensively replaced by epidote and chlorite), thus proving that the rock predates the high-pressure metamorphism. A striking feature is the widespread albite blastesis that obliterates any earlier fabric in the rock. Recent ideas suggest that this albite growth is due to ionic reactions during depressurization. In the presence of a Na^+ - and K^+ -rich fluid, the stability field of albite expands at the expense of mica during depressurization. It can be shown in the orthogneiss that the overall chemical composition remains relatively unchanged, so that the process was largely isochemical. On the other hand, albite growth may also be observed in the adjacent amphibole schists and gneisses, leading to so-called "spotted gneiss". Here metasomatism must have occurred. Because of the widespread growth of albite in both the basic and the acid rock, the contacts between them are often quite diffuse.

As we drive NE to the fishing village of Manzanillo, we will see basaltic dikes in the road cuts. A nice view can be had from the lookout with the arch. The cliffs below are called "Los Morros de Constanza". They probably have never been mapped.

Stop 1-4: SW end of Manzanillo Beach:

We are now standing in what Maresch (1971) originally mapped as the Manzanillo shear zone. Chevalier (1987) investigated the structure and interpreted the kinematics of the fault (Fig. 28), which he interprets as the result of a combination of both strike-slip movement and thrusting. Thirty years ago this outcrop could be examined in detail from below while walking along a sandy beach. Since then an estimated 5 meters or more of shore-line has been lost. A large slab of tectonized serpentinite hangs over the promontory separating us from the actual beach at Manzanillo. Many of the rocks around us are metasomatic black-wall products of reaction between serpentinite and more siliceous wall rock. The mineralogy here is predominantly chlorite and actinolite/tremolite with some fuchsitic green mica. However, elsewhere we can also find massive talc rocks as well as magnesite crystals up to several centimeters in size. In addition to metabasic rocks typical of the La Rinconada sequence we also find blocks of jet-black garnet-and/or epidote amphibolite. Are these the restites formed by anatexis of oceanic crust (e.g., Lázaro and García-Casco, 2008)? Fig. 29 is a particularly beautiful example of a coarse-grained epidote amphibolite from another locality at Cerro Chico. Taylor (1960), for lack of a better name, called such jet-black rocks with almost white epidote-mineral prisms up to 1-2 cm in length "pseudogabbros". Looking towards the NE we can see the continuation of the shear zone across the bay. Behind us in the hills the serpentinite-rich shear zone is marked by the dumps of workers digging for magnesite.

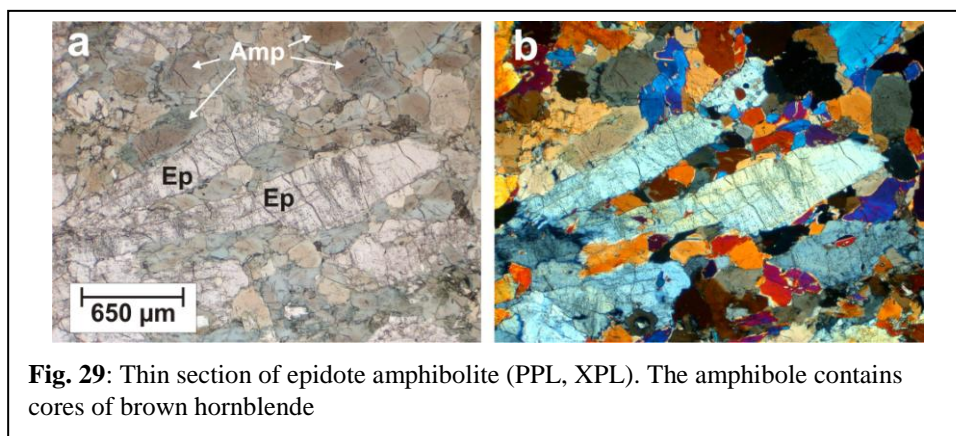


Fig. 29: Thin section of epidote amphibolite (PPL, XPL). The amphibole contains cores of brown hornblende

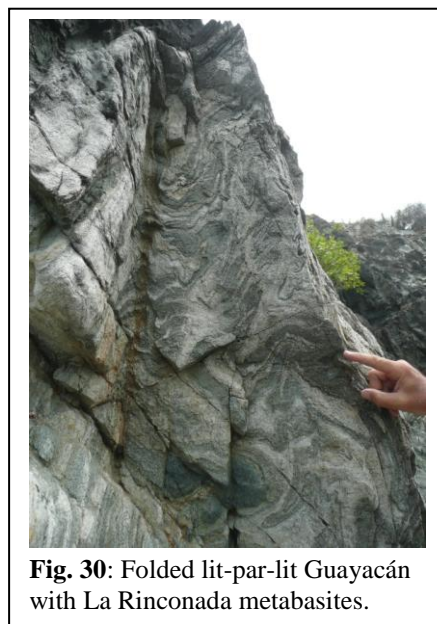


Fig. 30: Folded lit-par-lit Guayacán with La Rinconada metabasites.

Stop 1-5: NE end of Hotel Beach:

At the end of the beach leading NE from our hotel we will find an intriguing Guayacán/La Rinconada contact relationship that should be food for much discussion (Fig. 30). Lit-par-lit intercalations are ptymatically folded. Such features are not uncommon in the low hills south of Pedro González. Are these deformed anatexites in subducted oceanic crust?

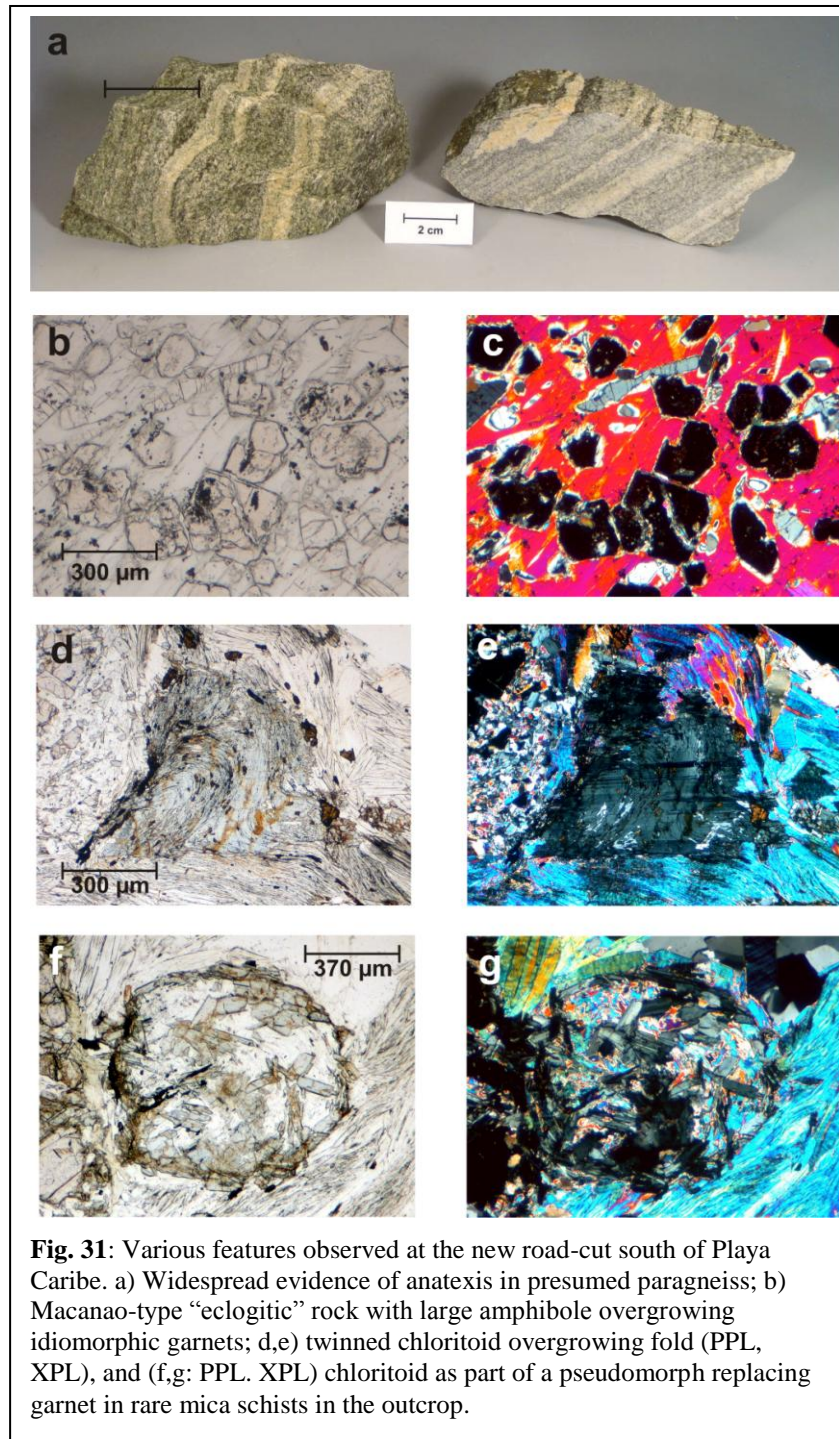
Stop 1-6: North flank of Cerro Chico (time permitting):

Good fresh outcrop of ultramafic rock will not be quickly accessible during our itinerary. A short drive into the valley east of Pedro González would allow us to sample dunite and pyroxenite in blocks, as well as black garnet amphibolites.

Day 2:

Stop 2-1: Fortin La Galera:

The old Spanish fort is built on sheared gneiss belonging to the lower unit PMjg1 of the JGMS. The fabric is conspicuously planar. A reconnaissance petrographical survey indicates widespread retrograde reactions involving the formation of biotite at the expense of white mica. Such reactions are common during pressure release in high-grade gneisses. Large idiomorphic crystals of late twinned chlorite cross-cutting the foliation have been observed. However, more detailed



study is needed to understand the many complex reaction relationships seen in thin section.

No doubt the most critical new data available from this outcrop are the zircon age data provided by Wright (pers. commun., 2010), which indicate Lower Cretaceous ages. The youngest detrital zircons have been dated at 129 Ma.

Stop 2-2: New road cut at Playa Caribe

Before turning to this new road-cut, it is worthwhile to examine the strongly interfolded graphitic and non-graphitic gneisses and schists only a few hundred meters away on the coast to the north. The contrasting nature of the distinctive planar gneissic fabric in the road-cut, very reminiscent of **stop 2-1**, is then immediately apparent. However, even more distinctive is the evidence for anatexis seen in these rocks (Fig. 31). If the Cretaceous ages at Fortin La Galera for the gneiss protolith are also applicable to these very similar gneisses, then it becomes difficult to escape the conclusion that anatexis occurred during the Cretaceous high-pressure

subduction-zone event. It is even more intriguing to speculate whether these anatectic magmas could be related to some of the granitic intrusives observed on the island.

The boudin of metabasic rock (Fig. 31) observed in the eastern part of the outcrop is part of a train of such Macanao-type eclogitic rocks extending south to the salt marshes near Juan Griego (see map, plate 1).

Stop 2-3: New road cut SW El Maco

A new exposure in the road leading from El Maco (also called Bolivar) to Boquerón allows insight into one of the more intriguing occurrences of Macanao-type eclogite. Chevalier (1987) identified kyanite eclogite in boulder fields along the old road and estimated peak metamorphic temperatures of ~ 700°C from garnet rims and Fe²⁺/Mg fractionation between garnet and matrix omphacite. He interpreted a klippe resting on PMjg1 autochthon in the inaccessible hills to the north as the source for the eclogite. New exposures now show that the eclogites actually occur in layers, in part boudinaged, folded in harmony with JGMS schists (Fig. 32). Black wall rocks are associated with the eclogite and indicate nearby serpentinite. The eclogites show distinctive features such as garnets with atoll structures (Fig. 33).

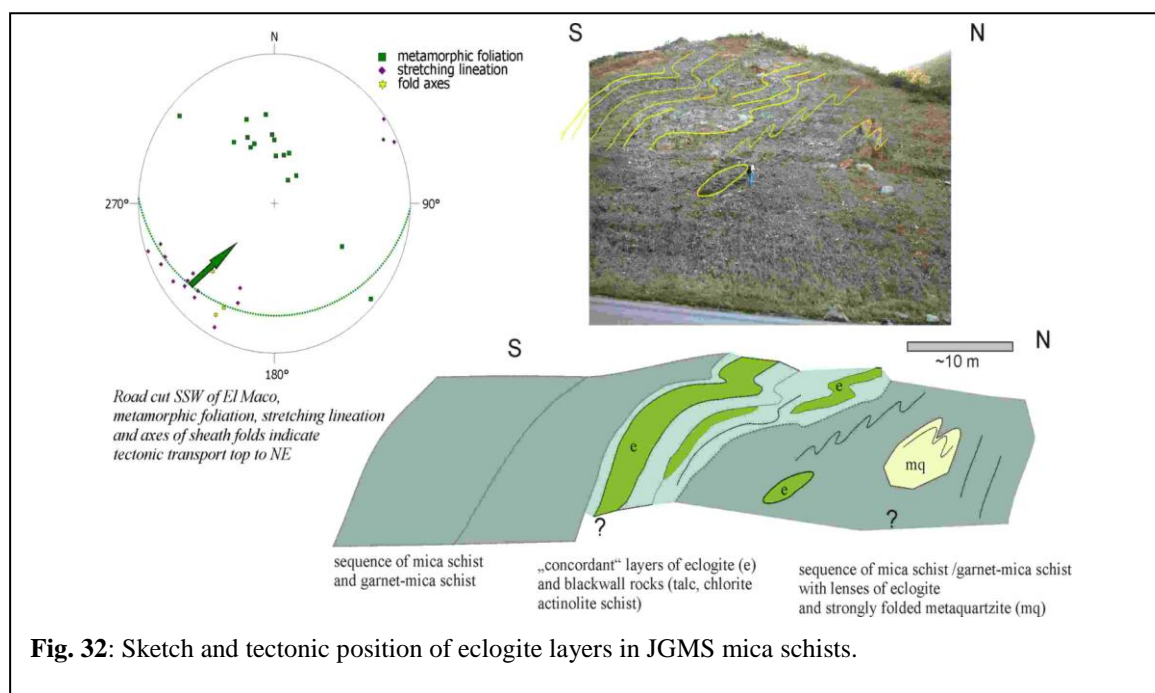
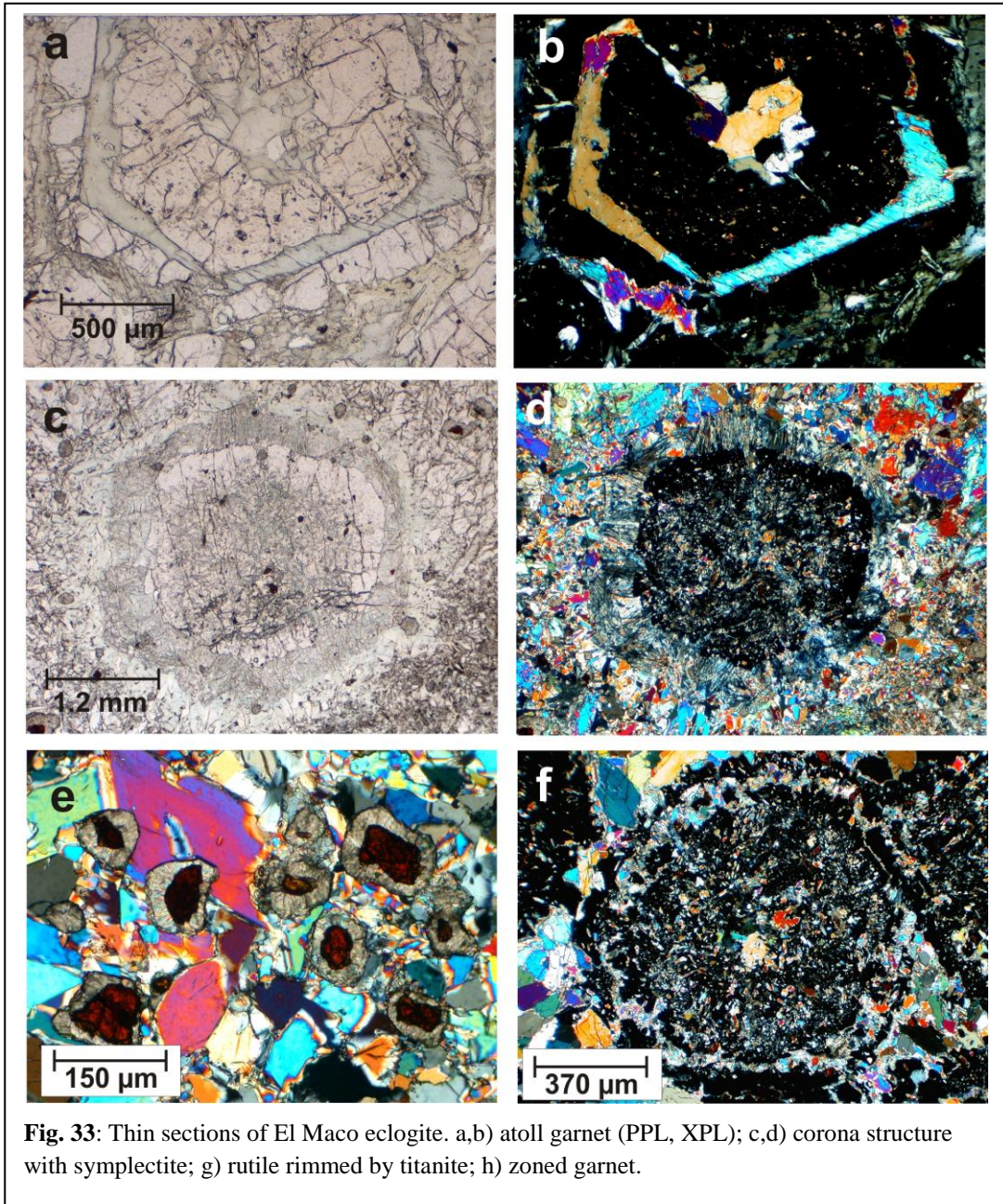


Fig. 32: Sketch and tectonic position of eclogite layers in JGMS mica schists.

Table 5: Initial Sr ratios of Margaritan orthogneisses.

RockType/Isochron	(⁸⁷ Sr/ ⁸⁶ Sr) _i
Guayacán Gneiss	
(WR/WM)	0.70296(2)
Matasiete Metatrandhemite	
(calculated on basis of U/Pb age)	0.70297
Ostos (1990)	0.70302-0.70344
El Salado Metagranite	
(WR/WM)	0.70893(3)
(WR/WM)	0.71030(5)
(WR/WM)	0.71036(18)
Macanao Orthogneiss	
(WR/WM)	0.71386(86)
(WR/WM)	0.71166(4)
(WR/WM)	0.71239(8)
El Maco granitic gneiss	
(WR/WM)	0.71817(4)
WR/WM = isochron based on whole rock/white mica; data from Kluge (1996) and Grafe (pers. commun.)	

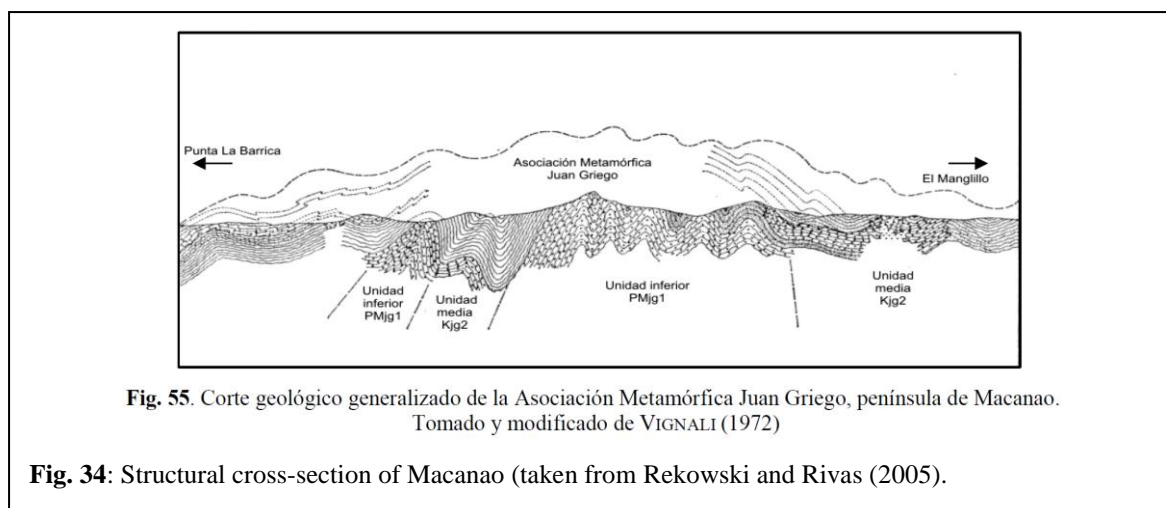
Downhill, towards the NNE, a leucocratic granitic gneiss is found interlayered with coarse-grained garnet-mica schist. A white-mica—dominated WR/WM isochron Rb/Sr on this material yields 82 ± 2 Ma, which could be cautiously interpreted as the age of intrusion, perhaps indicating affinity with the El Salado Metagranite. However, the initial, high Sr ratio (Table 5) is intriguing. The body may in fact be associated with the large San Juan Bautista Metagranite exposed just to the south (Plate 1), for which little data are available at present.



Day 3, Macanao Peninsula:

Stop 3-1: El Manglillo, south coast of Macanao

Starting from the sea-shore village of El Manglillo (or El Manguillo on some maps) we will walk directly northward for about 2 km along the top of a N-S ridge to an elevation of ~ 150m. This traverse will take us across unit Kjg2 of the Juan Griego Metamorphic Suite, indicated as predominantly graphitic mica schist on the map of Plate 1. This unit is considered to be the upper part of the JGMS section on Macanao (Fig. 34).



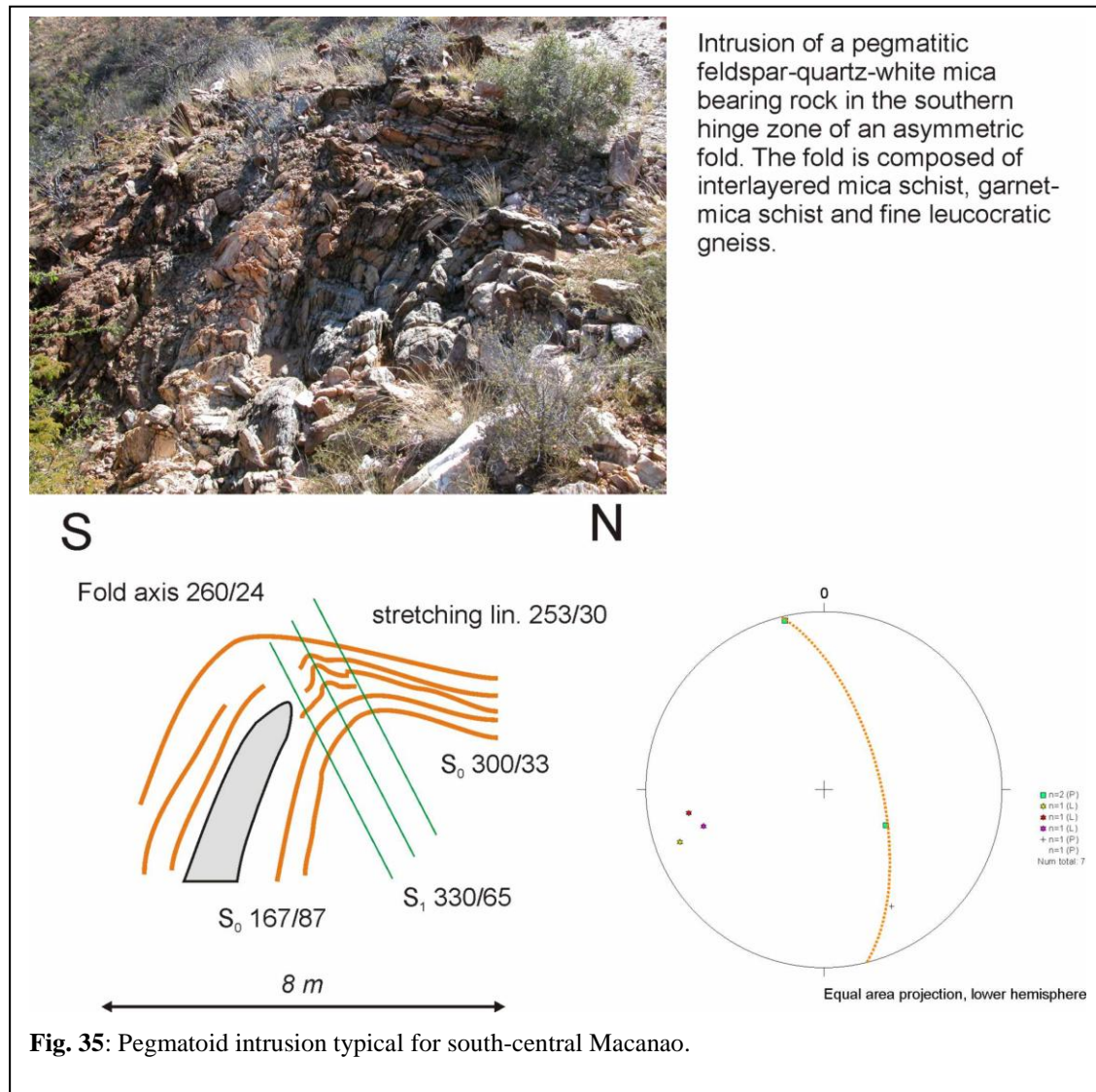
In detail, and in accordance with descriptions given by González de Juana and Vignali (1972) as well as Rekowski and Rivas (2005), the lithologies are more diverse. We will be walking across quartz-rich mica schists with the amount of graphitic material varying from 0 to 25%. Garnet may or may not be present, with grain sizes reaching 1 cm. Krückhans-Lueder (1996) described Al-rich varieties also containing staurolite and kyanite from a quebrada several hundred meters to the west, on which thermobarometric analysis was carried out (see Appendix B). Interbedded quartzites occur in layers generally < 50 thick. However, these also commonly occur grouped together to form thick resistant beds.

Although gneissic rocks predominate in the high hills of central Macanao, where they form the backbone of the central massif Fig. (34) they can also be found as mm- to dm-thick interlayers within the above sequence. These gneissic rocks have not been studied very systematically so far. Macsotay et al. (1997) give petrographic descriptions of a number of feldspar-rich samples, all of which they consider to be metasedimentary, despite the common occurrence of perthitic K-feldspar. Microanalytical data are not reported.

On the basis of the brief petrological overview of Kluge (1996) and Krückhans-Lueder (1996), who also present microanalytical data, the gneissic rocks of the JGMS on Macanao unit can be broadly differentiated into two types. One is an augengneiss with porphyroclasts of perthitic potassium feldspar that can be assumed to be an orthogneiss. Zircon from this rock type has been dated (Kluge, 1996; see Maresch et al. 2009), and more detailed mineralogical information is given in Appendix B. The second gneiss type lacks the typical porphyroclasts of perthitic potassium feldspar and is richer in quartz-rich schlieren and layers. Carbonaceous material is common. Depending on the amount of mica, the rocks can appear either compact or well-foliated with a distinct planar fabric. Plagioclase in most of these rocks is recrystallized albite with less than 4 mol% An-component. However, in some specimens porphyroclasts of an older generation are found that may reach oligoclase composition with 26 mol% An-content. Some contain helicitic whorls of graphite stringers with no relationship to the external foliation and conspicuous overgrowths of later albite. Gneisses with such porphyroclasts are often distinctly

grayish in colour. Some of these gneisses also contain larger plagioclase crystals choked with nests of epidote needles suggesting partial reequilibration of an originally more basic plagioclase indicative of a higher-grade origin of the original rock. A common feature of many of these rocks is the conspicuous growth of late porphyroblasts of albite that overgrow the fabric of the rock.

During our traverse we will also see an example (Fig. 35) of one of the numerous bodies of pegmatoid character in the south-central part of Macanao (González de Juana and Vignali 1972). These are described as apophyses typically from 50 cm to 10 m in diameter (Rekowski and Rivas, 2005) or thin sills up to 140 m. They are coarse-grained, with white mica reaching centimeter-size. Sodic plagioclase and quartz predominate. White mica may reach 10%. Perthite and graphic quartz—K-feldspar intergrowths have been noted. A Palaeocene to Early Eocene age has been suggested (Rekowski and Rivas (2005), in accordance with the presence of folding and brittle deformation but lack of metamorphic overprint.



We will encounter serpentinite bodies elongated parallel to the main foliation. Black garnet amphibolites with relict folds obliterated by the formation of pronounced axial-plane foliation in the surrounding mica schists are exposed in the overgrown quebrada to the west, but are not easily accessible. Hydrothermal vein quartz is abundant and forms a significant part of the regolith covering the ground.

During a field campaign in 2009, not only were the occurrences of quartzite found to be mineralogically diverse, containing pyroxene-, zoisite-, epidote-, and garnet, but in some cases massive layers consisting exclusively of garnet were also discovered (Fig. 36, 37). Quartzites often contain rusty pock-marks suggestive of considerable contents of former sulphides or other ore minerals that have been weathered away. These rocks pose intriguing questions as far as the original protolith is concerned. The garnetite is rose-coloured and forms concordant m-sized layers/boudins within metapelite country rock (Fig. 36, a,b). Garnets are subhedral, less than 2 mm in diameter (generally between 100 and 200µm) and sit in a quartz matrix (Fig. 36, c). Some garnets can be characterized by a distinctive zonation, already visible under the polarizing microscope (Fig. 36, g,h). Minor constituents of the rock are rutile, ilmenite, apatite, allanite and white K-mica. Allanite forms euhedral grains, in some cases also filling the interstices between garnet (Fig. 37, c,d). Dark-green mm-sized spots in the garnetite are due to interstitial chlorite (rather than quartz) between garnet grains (Fig. 36, e,f), possibly representing pseudomorphs. Some garnetites are quite rich in isometric apatite grains (which have the same grain-size as the associated garnets; see Fig. 36, d) leading to 8.5 wt.% P₂O₅ in some bulk-rock composition. The P-rich garnetites are generally also higher in CaO, Sr, Ce, La, Nd and lower in Al, Si, Zr, Nb, compared to their P-poorer (P₂O₅ = 0.07-1.96 wt.%) equivalents.

In general the garnets are quite rich in spessartine component, and their zonation is not very pronounced. Cores (typically Alm_{60.8}Gross_{4.5}Prp_{11.3}Spess_{19.2}And_{2.8}) are lower in grossular component compared to the rims (Alm_{59.3}Gross_{9.0}Prp_{9.0}Spess_{19.3}And_{1.4}), whereas pyrope, almandine and andradite are higher. The Si-content of white K-micas varies between 3.08 and 3.25 pfu. Ilmenites are characterized by appreciable amounts of pyrophanite component ((Fe_{0.72-0.87}Mn_{0.28-0.11})TiO₃); the geikielite component is negligible.

Garnets from the metapelitic country rock are generally much lower in spessartine component than in the adjacent garnetite. They show a pronounced zonation in that their cores are quite low in grossular (e.g. Alm_{77.5}Gross_{1.2}Prp_{13.1}Spess_{4.0}And_{2.4}), increasing markedly towards the rim (e.g. Alm_{62.6}Gross_{24.6}Prp_{6.4}Spess_{1.9}And_{2.2}).

Although there are various theories to explain the formation of such garnetites, in principle two main alternatives appear relevant here. The association of isometric grains of apatite with garnet appears to point to some kind of placer environment. This would be in agreement with the enclosing pelitic sediments. Alternatively, the protolith of the garnetite could represent a layer of Fe- and Mn-rich mud formed in a “black-smoker”-like volcanic environment within a submarine basin. Subsequent metamorphism could then have transformed the pelitic country rocks into garnet-mica schist and the Fe- and Mn-rich mud into garnetite. This kind of genesis (in part with minor modifications) is known from spessartine-rich garnetites (so-called “coticules”) of the Ardenne Mountains in Belgium (e.g. Kramm, 1976; Krosse and Schreyer, 1993). Likewise, Willner et al. (2001) describe similar rocks from the Coastal Cordillera Series in Central Chile. Those rocks are interpreted to have formed from ferriferous and manganiferous hydrothermal precipitates mixed with aluminous alteration-derived material, which became concentrated on top of the oceanic crust. Although the rocks described by Willner et al. (2001) are much higher in Si than the garnetites from Macanao, a typical feature for such an environment would be the strong deficiency in alkalis. However, the amount of the spessartine component in the Coticule garnets from Belgium and Chile is much higher (Spess_{>40}) than in the garnets described here (Spess_{<20}; composition see above).

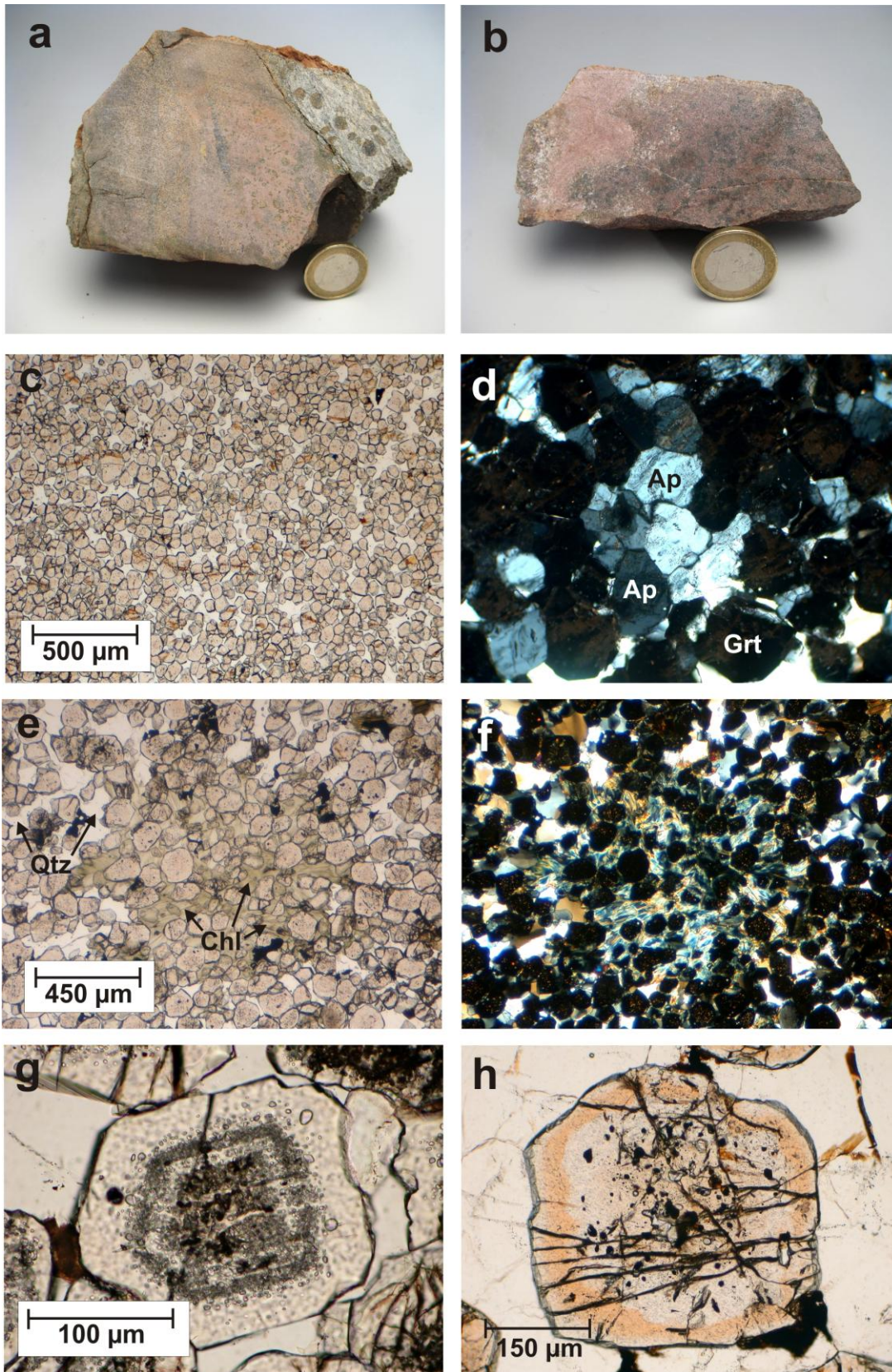


Fig. 36: Various features of garnetites occurring north of El Manglillo. a) Garnetite in sharp contact with graphitic garnet-mica schist; b) varicoloured garnetite, apatite-rich in lighter-coloured area; c) “sand-stone” aspect (PPL); intergrown apatite (XPL); d,e: chlorite pseudomorphs after ?? (PPL, XPL); g,h: distinctive zoning patterns of individual garnet grains.

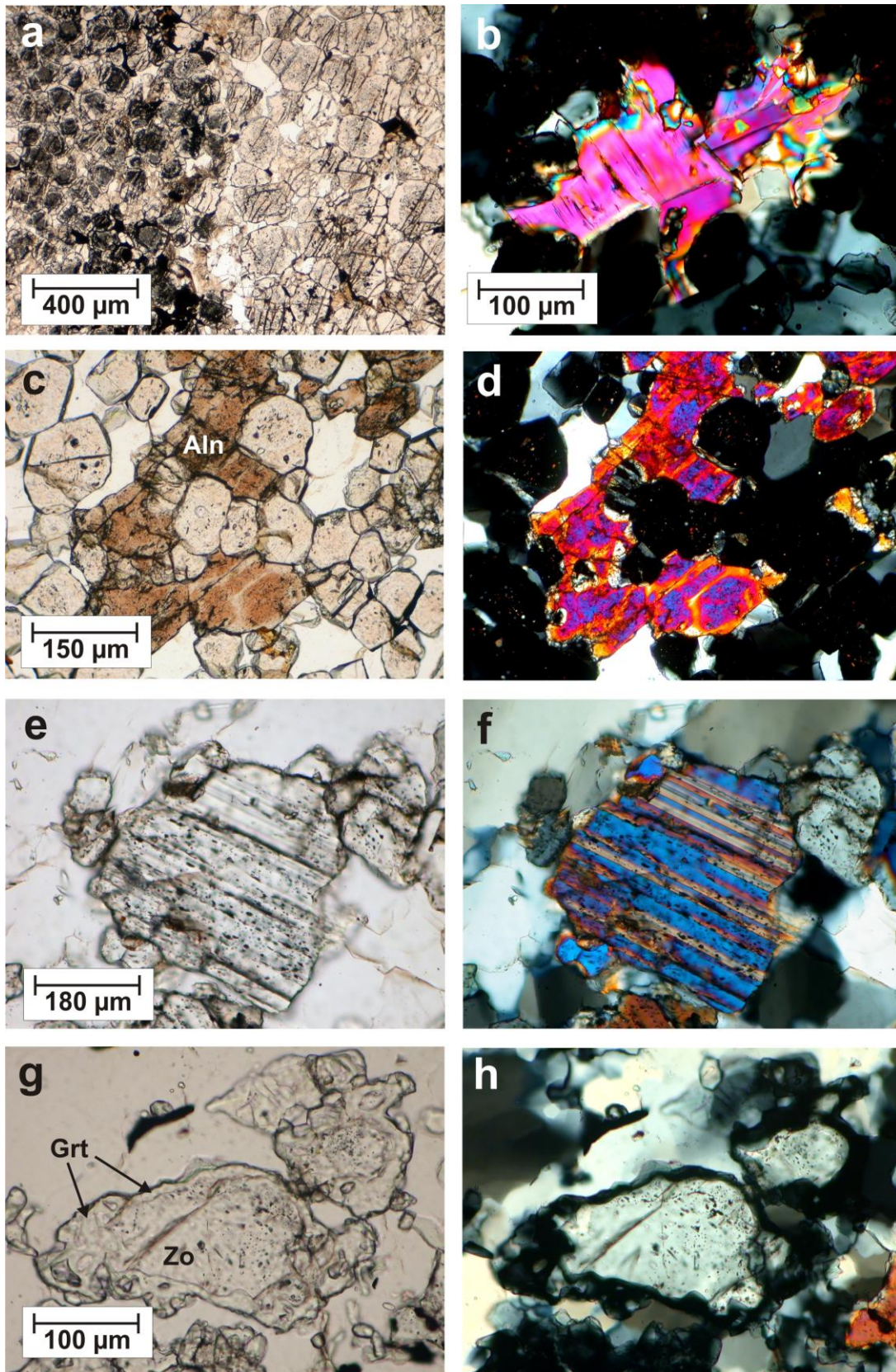


Fig. 37: Various features of garnetites and quartzites occurring north of El Manglillo. a) Contrasting garnet populations (PPL); b) intergrown phengite (XPL); c,d) intergrown allanite (PPL, XPL); e,f,) pyroxene crystal with lamellar structure in quartzite (PPL, XPL); d,h) zoisite crystal rimmed by overgrowth of garnet (PPL, XPL).

Stop 3-2: Robledal, NW Macanao

From the end of the road at Robledal, we will walk northwards to the old lighthouse, to a point now called Bajo Los Loros. We will be traversing unit Klr3, which is described as “meta-volcanosedimentary”, with metatuffs, graphitic schists and metapsammites. We will first encounter graphite-rich schists with a phyllitic aspect and no visible garnet. Nevertheless, Raman spectroscopy for two samples from this locality yielded high temperatures of 539 ± 38 and 569 ± 29 °C, suggesting that these rocks are actually strongly sheared phyllonites. These rocks probably mark a broad shear zone that can also be observed in mylonitized gabbro near El Maguey in NE Macanao. Several hundred meters further we will encounter light-coloured “pophyroids”, i.e. true low-grade probably dacitic metavolcanic rocks with porphyroclasts of feldspar set in a matrix of recrystallized quartz and newly-formed phengite, epidote and rare green (i.e. Fe-rich) biotite. Indicated metamorphic temperatures of ~ 400 °C are in strong contrast with the Raman results cited above.

On the north coast, at the foot of Morro de Robledal we will see a large body of greenschist-grade metagabbro (unit Mplr4) cut by a swarm of basaltic and doleritic dikes. Some general features of these dike swarms on Margarita are summarized in Fig. 38. A summary of unpublished geochemical and age data from the thesis of Kaiser (1996) is given in Table 6. Further published data on geochemistry may be found in Giunta et al. (2002) as well as Ostos and Sisson (2005). An affinity with island arc volcanic rocks appears likely.

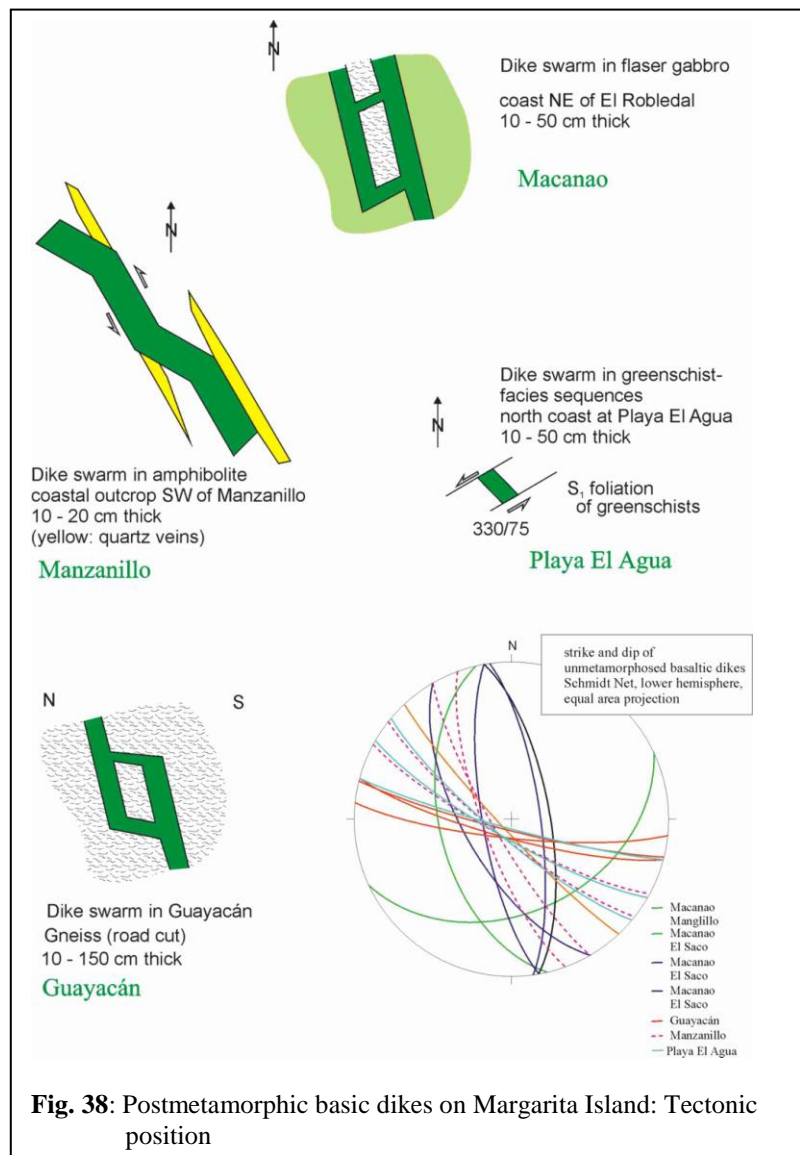


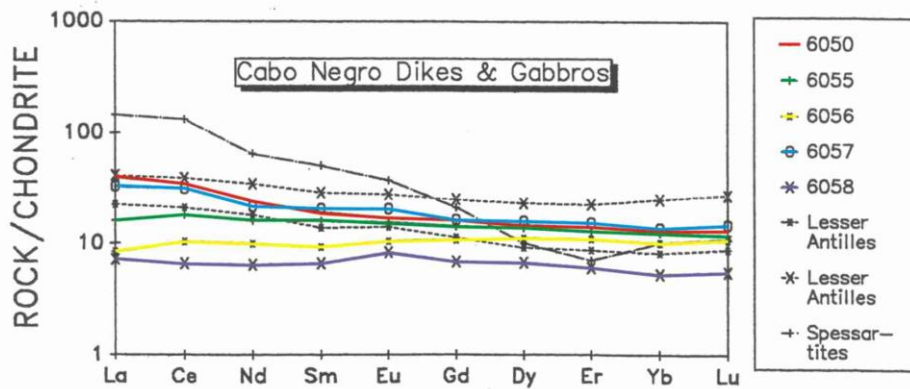
Fig. 38: Postmetamorphic basic dikes on Margarita Island: Tectonic position

Table 6: Postmetamorphic basic dikes on Margarita Island: Age data and REE patterns.

Ar/Ar ages of basaltic dikes cross-cutting the metamorphic units (ages in Ma). Considering the complex degassing patterns, the maximum intrusion ages are 38-40 Ma for the Macanao dikes, 55-43 Ma for the Cabo Negro and Manzanillo dikes, and 61 Ma for the Cabo Negro gabbro (Kaiser 1996).

Sample	Total Fusion age	Weighted Mean Plateau Age	Inverse Isochron Age	$^{40}\text{Ar} / ^{36}\text{Ar}$
6012 (Manzanillo)	51.66±19.6	49.39±49.39	45.35±12.74	305.8±33.5
6050 (Cabo Negro basaltic dike)	51.15±0.1	51.54±0.09	94.69±90.41	5607±2825
6055 (Cabo Negro gabbro)	66.09±0.15	66.26±0.15	66.29±3.29	330.9±58.5
6056 (Cabo Negro basaltic dike)	75.28±0.22	71.04±0.20	55.83±8.48	446.5±78.0
6501 (Macanao basaltic dike)	48.97±0.12	49.56±0.11	45.86±3.34	344.9±49.7
6507 (Macanao basaltic dike)	45.34±0.10	45.22±0.10	43.41±1.41	329.0±23.8

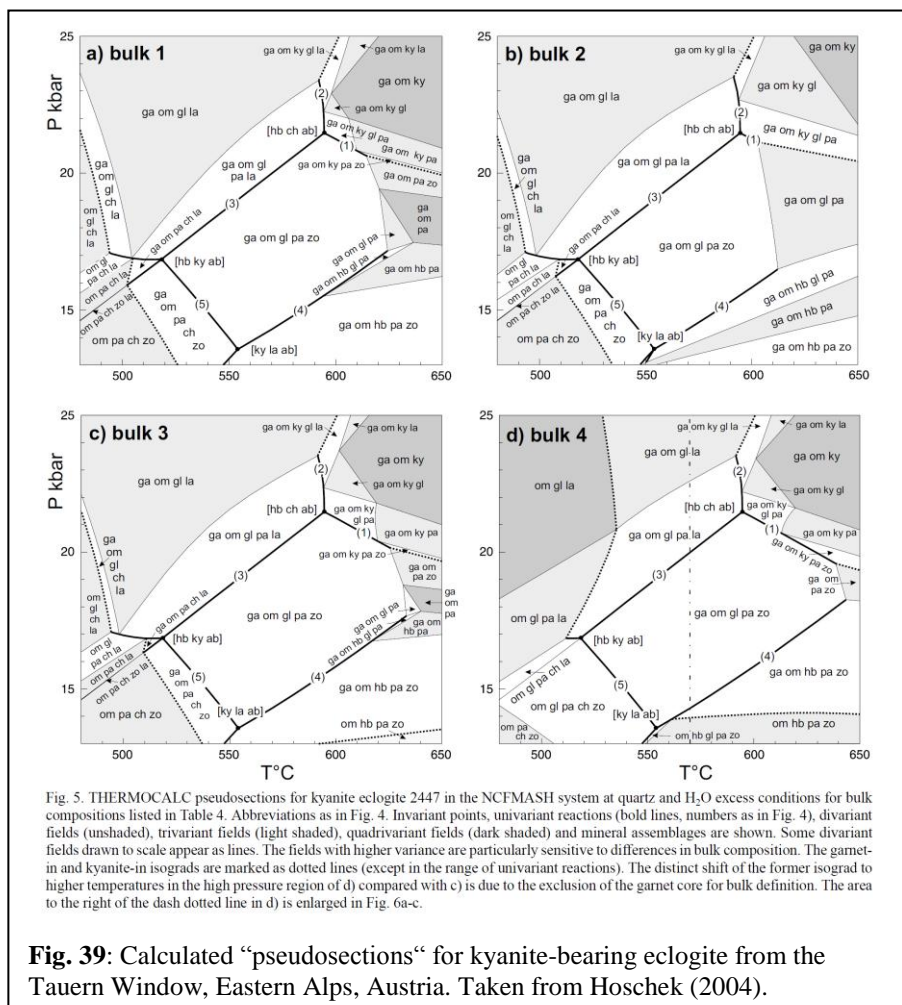
Chondrite normalized (Sun & McDonough 1989) REE pattern of Cabo Negro basaltic dikes and gabbro. All samples show uniform flat pattern without indication for magmatic differentiation (Kaiser 1996).



Stop 3-3a, 3b, 3c: Eclogite bodies in north-central Macanao

The purpose of these visits is to sample Macanao-type eclogites from the large Santa Inés body near the town of San Francisco as well as two occurrences of rare kyanite-bearing eclogites first reported by Navarro (1974) and described in Blackburn and Navarro (1977). The Ky-eclogites are located at Punta Tunal on the north coast and ~ 3.5 km ESE thereof. The significance of this rock type can be appreciated with an example from the Alps (Fig. 39). Although dependent on rock bulk composition, minimum pressures and temperatures for the appearance of kyanite are seen to be ~ 20 kbar and ~600 °C.

At La Pared, Navarro (1974) and Blackburn and Navarro (1977) report massive light-green and coarse-grained rocks with the assemblage garnet-clinopyroxene±zoisite-kyanite-paragonite-rutile±quartz±amphibole. At the second locality, Navarro (1974) reports Ky-eclogites that are very dark in colour, with porphyroblasts of garnet up to 4mm in size as the only macroscopically identifiable minerals. Kyanite crystals are evident on weathered surfaces. Kyanite and zoisite crystals may be up to 2 cm in length.



Stop 3-4 (time permitting). Las Tetras de Maria Guevara

Yes, Virginia, the name means exactly what you think. These twin hills in the broad flat plain between the two parts of Margarita have been a land-mark for sailors for many centuries, who are said to have lovingly named them after a particularly well-endowed local lass. This is a Venezuelan national monument and an interesting geological oddity. Early on these hills were mapped as volcanic cones. The map of Rekowski and Rivas (2005) indicates mainly JGMS with minor LRMS. We looked at them a few years ago and near the top of one of them we did indeed find brecciated rock in dark, glassy-looking matrix. Analyses quickly showed, however, that the

dark groundmass was mainly phosphatic. In other words, these hills probably once rose above a high-stand, shallow ocean and served as nesting grounds for birds. The reworked guano impregnated the brecciated schist and led to a hardened cap that protected them. At the moment we are looking for a palynologist to look at the pollen that should have survived the digestive and solution/redeposition process.

Day 4:

Stop 4-1: North end of Playa El Agua

Taylor (1960) originally called these rocks the “Manzanillo metavolcanic member”. They are now included in the PMC (Table 1) as “Metavolcánicas de Manzanillo”, although they are clearly of much lower grade than most of the PMC. The rocks are finely laminated, light-green to –brown siliceous schists of probable tuffaceous origin.. The silica occurs in thin (0.1 to 1.0 cm), discontinuous layers separated by chlorite or actinolite-rich laminae, or as discrete, dark-gray beds up to 10 cm thick. Weathering usually reduces the outcrops to low mounds of splintery, siliceous rubble. The variation in colour of these schists is due to different proportions of siliceous and chlorite-actinolite-epidote layers. Cross-cutting dikes are common.

The green-weathering schist is made up of a fine-grained matted intergrowth of acicular, light-green actinolite, yellow-green poikiloblastic epidote, sheaves of chlorite with minor biotite, and equidimensional grains of untwinned albite, all interspersed with lenticular aggregates of polycrystalline albite. Lenses of polycrystalline quartz are relatively sparse. The brown-weathering schists may contain up to 50% of 1 mm laminae of strained polycrystalline quartz. The rest of the rock is composed of finer-grained albite aggregates with interstitial chlorite, some biotite, and minor epidote. Carbonaceous material is common, but is most abundant in parallel streaks marking a crude but uniform foliation in the dark-gray, banded, siliceous layers, which have been recrystallized to fine-grained quartzites.

Stop 4-2: Punta Cabo Blanco

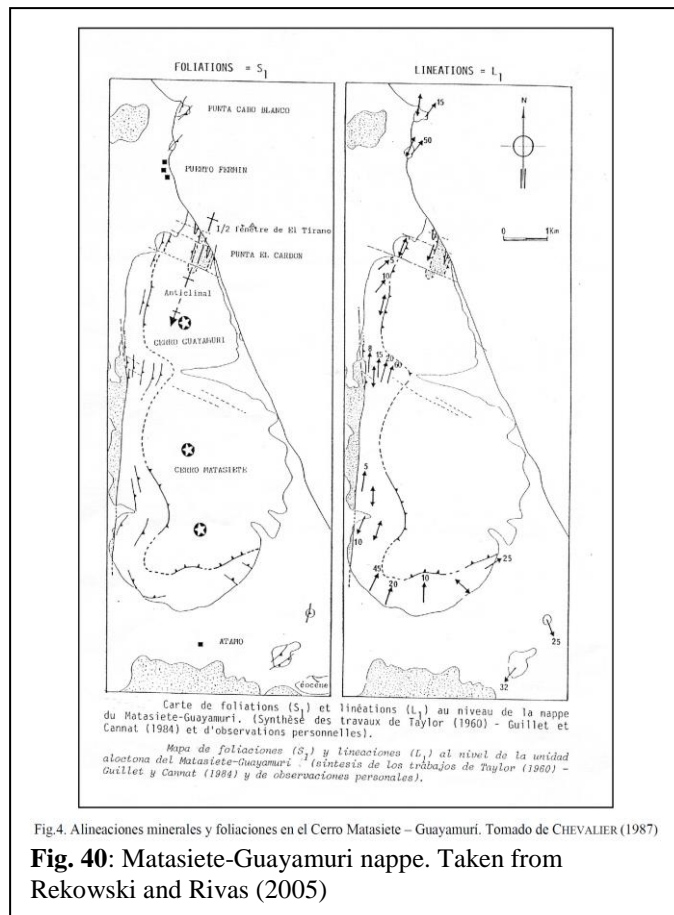
At this locality, over about 100 m, gabbro and diorite intrusions into La-Rinconada-type metabasic rocks make up over 90% of the outcrop. The brownish, strongly weathered La Rinconada rocks are sheared and retrogressed to a green-schist-facies mineralogy. Gabbro/diorite exhibits complex multiple intrusion relations, producing layers, from several centimeters to several meters thick, varying widely in grain size and occurring in sharp and complex mutual contact. All the rocks have been subjected to heterogeneous ductile deformation with enormous variations in strain gradients over only a few centimeters. Amphibole, in some cases also plagioclase, occurs as porphyroclasts (“augen”) up to 2 cm in size in a matrix of epidote/clinozoisite, secondary plagioclase/amphibole, white mica and chlorite. Minor quartz is present. Remnants of pyroxene are found in some amphibole porphyroclasts. The low outcrop at the beginning of the next beach to the south contains a heterogeneous assemblage of graphitic schist, garnet-mica schist, albite gneiss (similar to Guayacán Gneiss) and pods of of actinolitic black-wall rock.

Stop 4-3: Punta Montadero (Playa Parguito)

At this outcrop we are at the base of the Matasiete-Guayamuri nappe in sheared Matasiete Metatrandheimite (Fig. 40, 41).

This famous intrusion was already mentioned over 60 years ago by H.H. Hess (“Matasiete soda granite porphyry”). Its chemical analysis was quoted by Turner and Verhoogen in their early textbooks of the nineteen-sixties. Is it a plagiogranite (e.g. Navarro F., 1987; Stöckhert et al., 1995) related to MOR processes? Is it related to back-arc spreading processes (Navarro and

Ostos, 1997)? In both cases the Matasiete age would constrain the age of the oceanic crust formed and later subducted. Or were the Matasiete magmas formed by anatexis of subducting oceanic crust (Ostos and Sisson, 2005; Maresch et al., 2009)? In that case the Matasiete age would date the subduction process itself. Due to the distinct similarity of Matasiete and Guayacán rocks, any conclusion with respect to one should also apply to the other.



At the present locality (incorrectly called "Punta Cabo Blanco") in Fig. 40, mylonites and ultramylonites are beautifully developed (Fig. 42), and the change to a sheared but recognizable magmatic rock can be followed towards the south. In fact, it is very difficult to find Matasiete with a relict igneous fabric (Fig. 42).

We will make our way from here to a small group of houses called "Flandes" that lies nestled in the valley between the twin peaks of Cerro Guayamuri and Cerro Matasiete (Fig. 40). These peaks, as are almost all the high hills around, are underlain by ultramafics. The road to Flandes will wind up a steep escarpment caused by a relatively recent fault which beheads the valley we will be entering at the top. On the way up we will see sheared Matasiete Trondhjemite. The green chlorite-actinolite rocks in the white gneiss are former basic schollen and dykes in the intrusive.

Stop 4-4: East coast north of Punta Guacuco

A quick stop to collect samples of harzburgite in boulder deposits in the terraces. Care is advisable. Many peridotites contain deformed porphyroclasts of clinopyroxene that can mimic orthopyroxene in harzburgite.

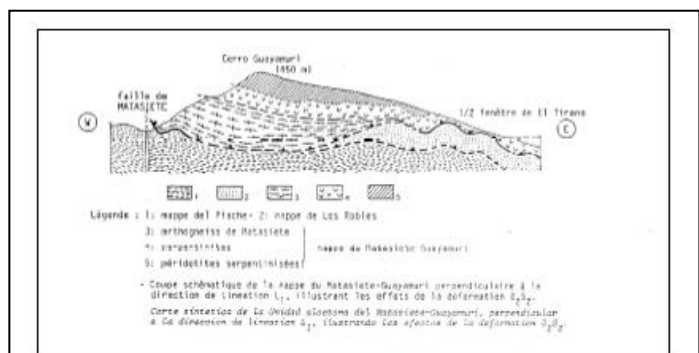


Fig. 19. Corte geológico de Cerro Guayamuri. Tomado de CHEVALIER (1987)

Fig. 41: Cross-section through the Matasiete-Guayamuri nappe. Taken from Rekowski and Rivas (2005).

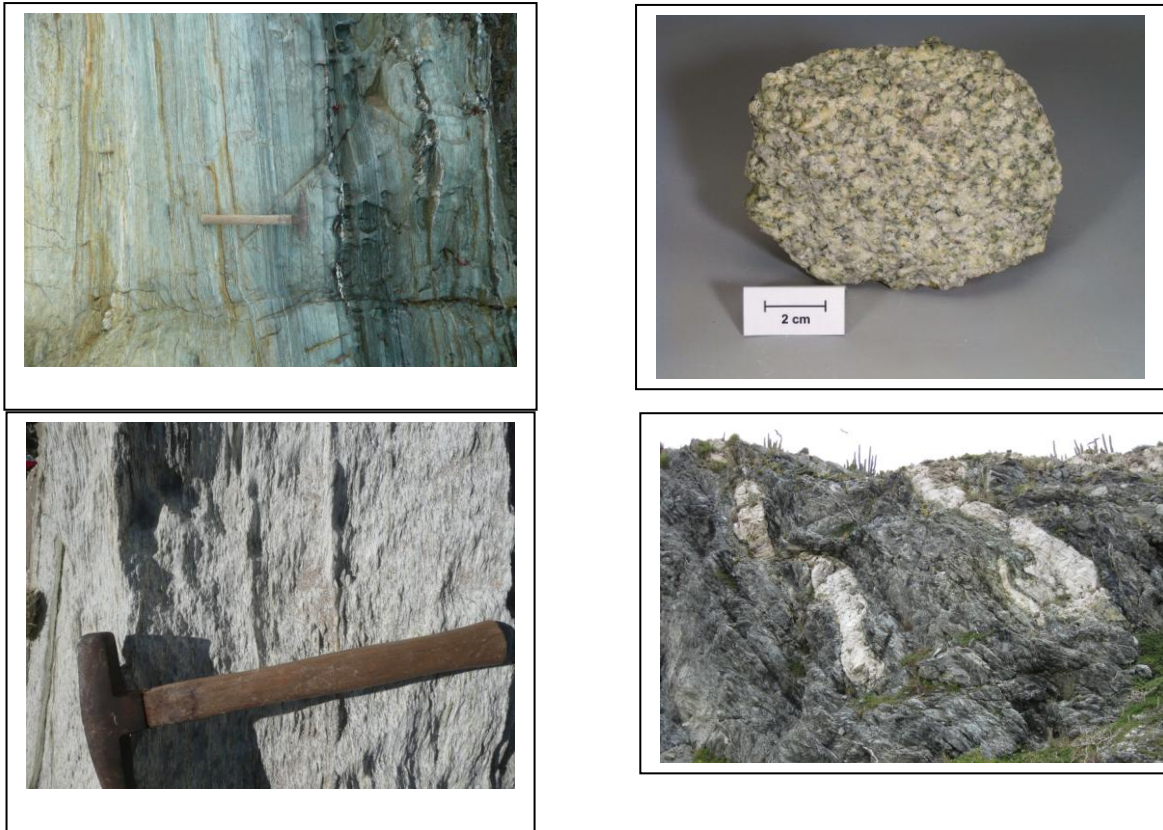


Fig. 42: Matasiete Metatrondhjemite (clockwise from lower left): ultramylonite; mylonite; equigranular intrusive; “cold-worked” tectonic fragments in serpentinite.

Stop 4-5: La Rinconada:

As this is being written, we have no knowledge of the present outcrop conditions at this locality. If all goes well, we may see La-Rinconada-type rocks of metamorphic zone I: spotted, fine-grained, bluish-green gneisses with mica porphyroblasts. We may also be able to see Guayacán Gneiss intrusions into both metabasites as well as into graphitic mica schists interlayered with the metabasic rocks.

Day 5:

Our plans for this last day are open to discussion. We tentatively envision a work-shop to summarize what we have seen, to discuss existing interpretations or propose new ones, and to try and fit our ideas into a general common view of the geodynamic development of the southern Caribbean. We may also want to go back in the field for further hands-on data collection.



INTERNATIONAL STRATIGRAPHIC CHART

International Commission on Stratigraphy

eon	era	system	epoch	stage	age Ma	GSSP
Phanerozoic	Cenozoic	Quaternary*	Holocene	Upper	0.0118	
			Pleistocene	Middle	0.126	
Phanerozoic	Cenozoic	Neogene	Pliocene	Lower	1.806	
				Gelasian	2.588	
				Placenzian	3.600	
			Miocene	Zanclean	5.332	
				Messinian	7.246	
				Tortonian	11.603	
		Oligocene	Serravallian	13.65		
			Langhian	15.97		
			Burdigalian	20.43		
		Eocene	Chattian	23.03		
			Rupelian	28.4 ± 0.1		
		Paleogene	Eocene	Priabonian	33.9 ± 0.1	
Bartonian	37.2 ± 0.1					
Paleogene	Eocene	Lutetian	40.4 ± 0.2			
		Ypresian	48.6 ± 0.2			
Paleogene	Eocene	Thanetian	55.8 ± 0.2			
		Selandian	58.7 ± 0.2			
Paleogene	Eocene	Danian	61.7 ± 0.2			
		Maastrichtian	65.5 ± 0.3			
Paleogene	Eocene	Campanian	70.6 ± 0.6			
		Santonian	83.5 ± 0.7			
Paleogene	Eocene	Coniacian	85.8 ± 0.7			
		Turonian	89.3 ± 1.0			
Paleogene	Eocene	Cenomanian	93.5 ± 0.8			
		Albian	99.6 ± 0.9			
Paleogene	Eocene	Aptian	112.0 ± 1.0			
		Barremian	125.0 ± 1.0			
Paleogene	Eocene	Hauterivian	136.4 ± 2.0			
		Valanginian	140.2 ± 3.0			
Paleogene	Eocene	Berriasian	145.5 ± 4.0			
Phanerozoic	Mesozoic	Cretaceous	Upper	145.5 ± 4.0		
			Lower	150.8 ± 4.0		
Phanerozoic	Mesozoic	Cretaceous	Middle	155.7 ± 4.0		
			Lower	161.2 ± 4.0		
Phanerozoic	Mesozoic	Cretaceous	Upper	164.7 ± 4.0		
			Middle	167.7 ± 3.5		
Phanerozoic	Mesozoic	Cretaceous	Lower	171.6 ± 3.0		
			Middle	175.6 ± 2.0		
Phanerozoic	Mesozoic	Cretaceous	Upper	183.0 ± 1.5		
			Middle	189.6 ± 1.5		
Phanerozoic	Mesozoic	Cretaceous	Lower	199.6 ± 0.6		
			Middle	203.6 ± 1.5		
Phanerozoic	Mesozoic	Cretaceous	Upper	216.5 ± 2.0		
			Middle	226.0 ± 2.0		
Phanerozoic	Mesozoic	Cretaceous	Lower	237.0 ± 2.0		
			Middle	245.0 ± 1.5		
Phanerozoic	Mesozoic	Cretaceous	Upper	248.7 ± 0.7		
			Middle	251.0 ± 0.4		
Phanerozoic	Mesozoic	Cretaceous	Lower	253.8 ± 0.7		
			Middle	260.4 ± 0.7		
Phanerozoic	Mesozoic	Cretaceous	Upper	265.3 ± 0.7		
			Middle	268.0 ± 0.7		
Phanerozoic	Mesozoic	Cretaceous	Lower	270.6 ± 0.7		
			Middle	275.6 ± 0.7		
Phanerozoic	Mesozoic	Cretaceous	Upper	284.4 ± 0.7		
			Middle	289.0 ± 0.8		
Phanerozoic	Mesozoic	Cretaceous	Lower	303.9 ± 0.9		
			Middle	306.5 ± 1.0		
Phanerozoic	Mesozoic	Cretaceous	Upper	311.7 ± 1.1		
			Middle	318.1 ± 1.3		
Phanerozoic	Mesozoic	Cretaceous	Lower	326.4 ± 1.6		
			Middle	345.3 ± 2.1		
Phanerozoic	Mesozoic	Cretaceous	Upper	359.2 ± 2.5		
			Middle	374.5 ± 2.6		
Phanerozoic	Mesozoic	Cretaceous	Lower	385.3 ± 2.6		
			Middle	391.8 ± 2.7		
Phanerozoic	Mesozoic	Cretaceous	Upper	397.5 ± 2.7		
			Middle	407.0 ± 2.8		
Phanerozoic	Mesozoic	Cretaceous	Lower	411.2 ± 2.8		
			Middle	416.0 ± 2.8		
Phanerozoic	Mesozoic	Cretaceous	Upper	421.3 ± 2.6		
			Middle	422.9 ± 2.5		
Phanerozoic	Mesozoic	Cretaceous	Lower	428.2 ± 2.4		
			Middle	428.2 ± 2.3		
Phanerozoic	Mesozoic	Cretaceous	Upper	436.0 ± 1.9		
			Middle	439.0 ± 1.6		
Phanerozoic	Mesozoic	Cretaceous	Lower	443.7 ± 1.5		
			Middle	445.8 ± 1.5		
Phanerozoic	Mesozoic	Cretaceous	Upper	455.8 ± 1.6		
			Middle	460.9 ± 1.6		
Phanerozoic	Mesozoic	Cretaceous	Lower	468.1 ± 1.6		
			Middle	471.8 ± 1.6		
Phanerozoic	Mesozoic	Cretaceous	Upper	478.6 ± 1.7		
			Middle	483.9 ± 1.7		
Phanerozoic	Mesozoic	Cretaceous	Lower	501.0 ± 2.0		
			Middle	542.0 ± 1.0		
Phanerozoic	Mesozoic	Cretaceous	Upper	542.0 ± 1.0		
			Middle			
Phanerozoic	Mesozoic	Cretaceous	Lower			
			Middle			
Phanerozoic	Mesozoic	Cretaceous	Upper			
			Middle			
Phanerozoic	Mesozoic	Cretaceous	Lower			
			Middle			
Phanerozoic	Mesozoic	Cretaceous	Upper			
			Middle			
Phanerozoic	Mesozoic	Cretaceous	Lower			
			Middle			
Phanerozoic	Mesozoic	Cretaceous	Upper			
			Middle			
Phanerozoic	Mesozoic	Cretaceous	Lower			
			Middle			
Phanerozoic	Mesozoic	Cretaceous	Upper			
			Middle			
Phanerozoic	Mesozoic	Cretaceous	Lower			
			Middle			
Phanerozoic	Mesozoic	Cretaceous	Upper			
			Middle			
Phanerozoic	Mesozoic	Cretaceous	Lower			
			Middle			
Phanerozoic	Mesozoic	Cretaceous	Upper			
			Middle			
Phanerozoic	Mesozoic	Cretaceous	Lower			
			Middle			
Phanerozoic	Mesozoic	Cretaceous	Upper			
			Middle			
Phanerozoic	Mesozoic	Cretaceous	Lower			
			Middle			
Phanerozoic	Mesozoic	Cretaceous	Upper			
			Middle			
Phanerozoic	Mesozoic	Cretaceous	Lower			
			Middle			
Phanerozoic	Mesozoic	Cretaceous	Upper			
			Middle			
Phanerozoic	Mesozoic	Cretaceous	Lower			
			Middle			
Phanerozoic	Mesozoic	Cretaceous	Upper			
			Middle			
Phanerozoic	Mesozoic	Cretaceous	Lower			
			Middle			
Phanerozoic	Mesozoic	Cretaceous	Upper			
			Middle			
Phanerozoic	Mesozoic	Cretaceous	Lower			
			Middle			
Phanerozoic	Mesozoic	Cretaceous	Upper			
			Middle			
Phanerozoic	Mesozoic	Cretaceous	Lower			
			Middle			
Phanerozoic	Mesozoic	Cretaceous	Upper			
			Middle			
Phanerozoic	Mesozoic	Cretaceous	Lower			
			Middle			
Phanerozoic	Mesozoic	Cretaceous	Upper			
			Middle			
Phanerozoic	Mesozoic	Cretaceous	Lower			
			Middle			
Phanerozoic	Mesozoic	Cretaceous	Upper			
			Middle			
Phanerozoic	Mesozoic	Cretaceous	Lower			
			Middle			
Phanerozoic	Mesozoic	Cretaceous	Upper			
			Middle			
Phanerozoic	Mesozoic	Cretaceous	Lower			
			Middle			
Phanerozoic	Mesozoic	Cretaceous	Upper			
			Middle			
Phanerozoic	Mesozoic	Cretaceous	Lower			
			Middle			
Phanerozoic	Mesozoic	Cretaceous	Upper			
			Middle			
Phanerozoic	Mesozoic	Cretaceous	Lower			
			Middle			
Phanerozoic	Mesozoic	Cretaceous	Upper			
			Middle			
Phanerozoic	Mesozoic	Cretaceous	Lower			
			Middle			
Phanerozoic	Mesozoic	Cretaceous	Upper			
			Middle			
Phanerozoic	Mesozoic	Cretaceous	Lower			
			Middle			
Phanerozoic	Mesozoic	Cretaceous	Upper			
			Middle			
Phanerozoic	Mesozoic	Cretaceous	Lower			
			Middle			
Phanerozoic	Mesozoic	Cretaceous	Upper			
			Middle			
Phanerozoic	Mesozoic	Cretaceous	Lower			
			Middle			
Phanerozoic	Mesozoic	Cretaceous	Upper			
			Middle			
Phanerozoic	Mesozoic	Cretaceous	Lower			
			Middle			
Phanerozoic	Mesozoic	Cretaceous	Upper			
			Middle			
Phanerozoic	Mesozoic	Cretaceous	Lower			
			Middle			
Phanerozoic	Mesozoic	Cretaceous	Upper			
			Middle			
Phanerozoic	Mesozoic	Cretaceous	Lower			
			Middle			
Phanerozoic	Mesozoic	Cretaceous	Upper			
			Middle			
Phanerozoic	Mesozoic	Cretaceous	Lower			
			Middle			
Phanerozoic	Mesozoic	Cretaceous	Upper			
			Middle			
Phanerozoic	Mesozoic	Cretaceous	Lower			
			Middle			
Phanerozoic	Mesozoic	Cretaceous	Upper			
			Middle			
Phanerozoic	Mesozoic	Cretaceous	Lower			
			Middle			
Phanerozoic	Mesozoic	Cretaceous	Upper			
			Middle			
Phanerozoic	Mesozoic	Cretaceous	Lower			
			Middle			
Phanerozoic	Mesozoic	Cretaceous	Upper			
			Middle			
Phanerozoic	Mesozoic	Cretaceous	Lower			
			Middle			
Phanerozoic	Mesozoic	Cretaceous	Upper			
			Middle			
Phanerozoic	Mesozoic	Cretaceous	Lower			
			Middle			
Phanerozoic	Mesozoic	Cretaceous	Upper			
			Middle			
Phanerozoic	Mesozoic	Cretaceous	Lower			
			Middle			
Phanerozoic	Mesozoic	Cretaceous	Upper			
			Middle			
Phanerozoic	Mesozoic	Cretaceous	Lower			
			Middle			
Phanerozoic	Mesozoic	Cretaceous	Upper			
			Middle			
Phanerozoic	Mesozoic	Cretaceous	Lower			
			Middle			
Phanerozoic	Mesozoic	Cretaceous	Upper			
			Middle			
Phanerozoic	Mesozoic	Cretaceous	Lower			
			Middle			
Phanerozoic	Mesozoic	Cretaceous	Upper			
			Middle			
Phanerozoic	Mesozoic	Cretaceous	Lower			
			Middle			
Phanerozoic	Mesozoic	Cretaceous	Upper			
			Middle			
Phanerozoic	Mesozoic	Cretaceous	Lower			
			Middle			
Phanerozoic	Mesozoic	Cretaceous	Upper			
			Middle			
Phanerozoic	Mesozoic	Cretaceous	Lower			
			Middle			
Phanerozoic	Mesozoic	Cretaceous	Upper			
			Middle			
Phanerozoic	Mesozoic	Cretaceous	Lower			
			Middle			
Phanerozoic	Mesozoic	Cretaceous	Upper			
			Middle			
Phanerozoic	Mesozoic	Cretaceous	Lower			
			Middle			
Phanerozoic	Mesozoic	Cretaceous	Upper			
			Middle			
Phanerozoic	Mesozoic	Cretaceous	Lower			
			Middle			
Phanerozoic	Mesozoic	Cretaceous	Upper			
			Middle			
Phanerozoic	Mesozoic	Cretaceous	Lower			
			Middle			
Phanerozoic	Mesozoic	Cretaceous	Upper			
			Middle			
Phanerozoic	Mesozoic	Cretaceous	Lower			
			Middle			
Phanerozoic	Mesozoic</					

Appendix A (CD in pocket):

Rekowski F, Rivas L. (2005) Integración geológica de la isla de Margarita, estado Nueva Esparta. *Geos*, UCV, Caracas, 38: 97-98 (+ 242 p. and 18 maps in CD).

Appendix B:

Maresch WV, Kluge R, Baumann A, Pindell J, Krückhans-Lueder G, Stanek KP (2009) The occurrence and timing of high-pressure metamorphism on Margarita Island, Venezuela: a constraint on Caribbean –South America interaction. *In: James, K.H., Lorente M.A. & Pindell, J.L. (eds) The Origin and Evolution of the Caribbean Plate, Geological Society of London Special Publication, 328, 705-741.*

